Ultrasonics Sonochemistry 78 (2021) 105749

Contents lists available at ScienceDirect

Ultrasonics Sonochemistry

journal homepage: www.elsevier.com/locate/ultson

Synergistic effect of sonication on photocatalytic oxidation of pharmaceutical drug carbamazepine

Gizem Yentür , Meral Dükkancı *

Ege University, Engineering Faculty, Chemical Engineering Department, 35100 Bornova, Izmir, Turkey

ARTICLE INFO

Keywords:
Sono-photocatalytic
Synergistic effect
Continuous mode sonication
Pulse mode sonication
Pharmaceutical drug
Carbamazepine

ABSTRACT

Photocatalytic, sono-photocatalytic oxidation of pharmaceutical drug of carbamazepine was successfully carried out using Ag/AgCl supported $BiVO_4$ catalyst. For this purpose, firstly, photocatalytic oxidation was optimized by central composite design methodology and then synergistic effect of sonication was investigated. Low frequency (20 kHz) probe type and high frequency (850 kHz) plate type sonication at pulse and continuous mode were studied to degrade the carbamazepine (CBZ) containing wastewater. Pulse duties of 1:5 and 5:1 (on : off) were tested using the high frequency sonication system in the sono-photocatalytic oxidation of CBZ. The effects of frequency, power density measured from calorimetry by changing amplitudes were discussed in the sono-photocatalytic oxidation of CBZ. Complete carbamazepine removal was achieved at the optimum conditions of 5 ppm CBZ initial concentration with 1.5 g/L of catalysts loading and at an alkaline pH of 10 at the end of 4 h of photocatalytic reaction under visible LED light irradiation. Both low frequency and high frequency sonication systems caused an increase in photocatalytic efficiency in a shorter treatment time of 60 min. CBZ removal increased from 44% to 65.42% in low frequency sonication of 20 kHz at the amplitude of 20% (0.15 W/mL power density). In the case of high frequency ultrasonic system (850 kHz), CBZ removal increased significantly from 44% to 89.5 % at 75% amplitude (0.12 W/mL power density) within 60 min of reaction. Continuous mode sonication was observed to be more effective than that of pulse mode sonication not only for degradation efficiency and also for electrical energy consumption needed to degrade CBZ. Sono-catalytic oxidation was also conducted with simulated wastewater that contains SO_4^{2-}, CO_3^{2-}, NO^{3-}, Cl^- anions and natural organic component of fulvic acid. The CBZ degradation was inhibited slightly in the presence of NO_3^- and Cl^-, and fulvic acid, however, the existence of SO_4^{2-} and CO_3^{2-} increased the degradation degree of CBZ. Toxicity tests were performed to determine the toxicity of untreated CBZ, and treated CBZ by photocatalytic, and sono-photocatalytic oxidations.

1. Introduction

Rapid industrial development and population growth have led to serious environmental pollution and energy crisis. Water pollution is among the primary problems that need to be solved due to the presence of various wastewater from the food, textile, cosmetic, rubber, plastic (that use bisphenol A) and pharmaceutical industries due to their toxicity and non-biodegradation [1,2]. Pharmaceutical drugs are used to treat of illness, however a small amount of it is absorbed by the body tissues, most of it is given to sewers. As the, sewage treatment plants are effective for biodegradable wastes, aquatic environments from surface water to drinking water includes pharmaceutical wastes [3]. As a pharmaceutical drug, carbamazepine (CBZ) is well-known antiepileptic psychiatric drugs consumed worldwide for treatment of mood related disorders and have broad pharmaceutical applications. Major source of pharmaceuticals disposed in environmental systems are unabsorbed amount from human body in the sewage, improper disposal of unwanted/expired pharmaceuticals, and disposal of untreated and ineffectively treated wastewater [4]. Carbamazepine is hardly biodegradable (<10%) and conventional methods of treatment (biological treatment) do not adequately remove carbamazepine and other drugs from treated water. Therefore, these pharmaceutical compounds easily pass through the conventional wastewater treatment plants (WWTP), and enter the environment through the discharge of effluents, thus contaminating both surface and groundwater and contributing to environmental pollution which affects the local ecosystem, human

* Corresponding author.
E-mail address: meral.dukkanci@ege.edu.tr (M. Dükkancı).

https://doi.org/10.1016/j.ultsonch.2021.105749
Received 14 September 2020; Received in revised form 28 July 2021; Accepted 2 September 2021
Available online 6 September 2021

health and all living organism. The need for effective removal of pharmaceuticals has resulted in the emergence of effective, economic and environmentally friendly method such as advanced oxidation processes [5] through the production of powerful oxidizing agents like hydroxyl ($OH^{\cdot}$) and superoxide radicals ($O_2^{\cdot-}$). Photocatalytic oxidation and sonication are the example of advanced oxidation processes.

Sonication involves sonochemical reactions caused by ultrasound. Ultrasound involves sound waves with a frequency higher than that of human hearing (above 20 kHz). In sonochemistry ultrasound can be divided into two ranges, the range of 2 – 10 MHz is mostly used in the medical field, and the range of 20 kHz–2 MHz is utilized to influence chemical processes and reactions by producing cavitation in liquids [1,6]. Acoustic cavitation process caused by continuous or pulsed ultrasound waves involves the formation, growth and implosive collapse of tiny bubbles in a liquid at very small time intervals, which consequently produce chemical effects. The collapse of cavitation causes local hot spots at a pressure higher than 500 atm and temperatures as high as 5200 K in cavitation bubble and about 1900 K in the interfacial region between the solution and the cavitation bubble. These hot spots not only provide sufficient heat to degrade organic pollutants (thermolysis), they also dissociate water, forming hydroxyl radicals and initiate oxidation reactions in water [7–14]. The other effect occurs when ultrasonic waves pass through a liquid is acoustic streaming (time- independent fluid flow) [6]. There are three zones in sonochemical reactions: first one is the center of the cavitation bubble where the hydrophobic and volatile molecules are degraded due to the high temperature, and the active radicals form due to the pyrolysis of water, second one is the gas liquid interface where the oxidation reaction occurs by radicals formed in the cavitation bubbles, and the last one is the bulk solution where the oxidation reactions occur by radicals that escape form the interface [15]. However, sonolysis is an efficient process for the degradation of hydrophobic pollutants, its efficiency is weak for hydrophilic compounds. In addition to this, reaction volume and longer reaction time are the other obstacles which make the sonication ineffective when use as a single method.

The energy use are the most important agenda of conscious societies. The energy is a vital contribution for the financial development of a country and environmental quality. As known well, using fossil fuels as energy raises the amount of carbon dioxide (CO_2) emission which is a major cause of climate change and global warming. Therefore, it is an urgent necessity for renewable energy sources to replace fossil sources. Renewable energy sources includes sunlight, wind, tides, hydro, geothermal heat and biofuels. Among these, solar energy (sun light) is abundantly available at free of cost and adjustable to numerous applications [9]. For example solar energy can be utilized by photocatalysts to degrade organic pollutants, reduce CO_2 into renewable hydrocarbon solar fuels and for the production of hydrogen by water splitting [16,17]. In this concern, effort has been made for developing highly active visible light active heterogeneous photocatalysts for environmental applications in recent years [18]. Among them, Ag/AgCl composite has been widely applied to photocatalytic process due to the surface plasmon resonance effect of metallic Ag nanoparticles under visible light irradiation [19]. Semiconductor with Ag/AgCl can elevates the separation of electrons and holes [20]. However, there are some major limitations of the Ag/AgCl in practical applications, such as, separation difficulty from treated water, unstability under light irradiation (photo-corrosion), and agglomeration [19,21,22]. In order to overcome these limitations of Ag/AgCl and enhance the degradation of carbamazepine under visible light, AgCl was coupled with monoclinic scheelite bismuth vanadate (m-$BiVO_4$) which is considered as promising visible light driven photocatalyst due to its band gap energy value of 2.4 eV ($\lambda < 520$ nm) [23 –28]. Monoclinic bismuth has an edge over common use because of achieving efficient charge separation on different crystal facets which provides reduction reaction with photogenerated electrons and oxidation reaction with photogenerated holes, which take place separately on different facets under photo-irradiation [29].

Sono-photocatalysis is the hybrid process which use the combination of light energy, sonication and catalysis. The sono-photocatalytic process of oxidation shows interesting advantages at kinetic level, due to the presence of synergistic effect between sonolysis and photocatalysis [30,31]. Synergistic effect can be observed when reaction rate constant of sono-photocatalytic oxidation ($k_{Vis+US+Catalyst}$) is higher than that of the sum of reaction rate constants of sono-catalytic ($k_{US+Catalyst}$) and photocatalytic oxidation ($k_{Vis+Catalyst}$) [8,32]. Sonication is an efficient process for the degradation of hydrophobic pollutants in cavitation bubble and/or interface. On the other hand, photocatalytic oxidation is an efficient process for the degradation of hydrophilic compounds in the bulk solution since they can adsorb onto the polar catalytic surface. Thus, the hybrid process of sonocatalysis and photocatalysis, sono-photocatalysis, would overcome the obstacles of the individual processes. In addition to this, acoustic cavitation process would clean the surface of photocatalyst cause regenerating the active sites, and also cavitation bubbles would act as a nucleation site hence increase the number of bubbles [15,31].

The aim of the present work is to study the degradation of carbamazepine under visible light irradiation over plasmonic composite photocatalyst of Ag/AgCl/$BiVO_4$ and to investigate the effect of sonication on photocatalytic oxidation. For this purpose firstly photocatalytic oxidation of CBZ was optimized with parametric study and then sono-photocatalytic hybrid process efficiency was tested. High frequency (850 kHz) at pulsed and continuous modes and low frequency (20 kHz) sonication were used as sonication sources. In literature there are several studies on hybrid process of sono-catalytic/sono-photocatalytic oxidation under continuous mode of ultrasound [30,33 –40], a few studies on pulse mode sonication [41,42] and very few studies on comparison of pulse and continuous mode sonication [14]. However, the present study focuses on the degradation of carbamazepine by sono-photocatalytic hybrid process using low (20 kHz) and high (850 kHz) frequencies on both continuous and pulse modes. By changing the amplitudes values of both equipment, effect of power densities were also investigated at both low and high frequencies. Sono-catalytic runs were also performed using simulated waste water that contains inorganic ions of Cl^-, NO_3^-, CO_3^{2-}, SO_4^{2-} and natural organic component of fulvic acid. The efficiency of sonication on photocatalytic oxidation was not only discussed for the degradation of CBZ but also for economic efficiency. Toxicity tests were performed to determine the toxicity of untreated CBZ, and treated CBZ solution using photocatalytic and sono-photocatalytic oxidation.

In addition to all these, in the current study the $BiVO_4$ supported Ag/AgCl photocatalyst which showed excellent efficiency in photocatalytic oxidation at > 400 nm wavelength has been used for the first time as a catalyst for sono-catalytic and sono-photocatalytic study.

2. Experimental study

2.1. Preparation Ag/AgCl/$BiVO_4$

The plasmonic composite photocatalyst of Ag/AgCl/BiVO4 was successfully synthesized by two steps. In the first step, Ag NPs were selectively deposited on the (0 4 0) crystal plane of $BiVO_4$ in the presence of ammonium oxalate by photoreduction under visible LED light irradiation. Here, ammonium oxalate was used as hole scavenger agent, that let the reaction of electrons and Ag^+ in $AgNO_3$. In the second step, formed Ag NPs were oxidized by $FeCl_3$ to form Ag/AgCl. The catalyst preparation method was given in detail in the previous study [43]. Fig. 1 presents the schematic diagram of the catalyst preparation steps.

The prepared catalyst was characterized by XRD, XPS, SEM and nitrogen adsorption studies in previous study [43]. XRD studies confirmed the formation of monoclinic phase of $BiVO_4$. Along with XRD analysis, XPS analysis was also showed the presence Ag NPs and AgCl in the structure. The SEM images showed the morphology of $BiVO_4$ sample that was in the decagonal crystal structure. Before photodeposition of Ag

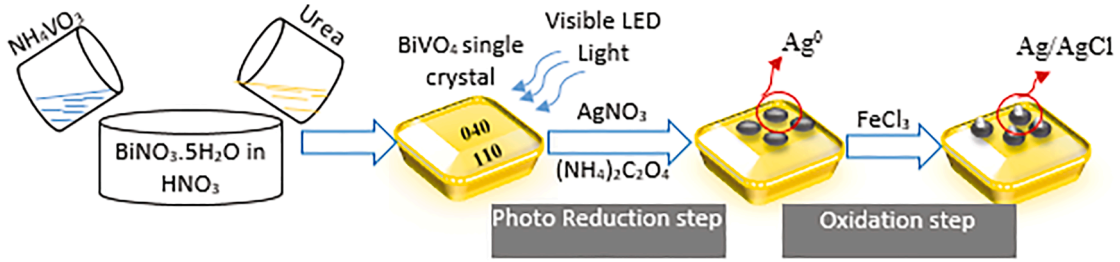

Fig. 1. Schematic diagram of catalyst preparation.

NPs on the (040) facet of monoclinic $BiVO_4$, the surface of $BiVO_4$ was smooth. After photoreduction, the deposition of Ag NPs on the surface was seen clearly. According to UV–Vis DRS analysis, the band gap energies of AgCl, $BiVO_4$, Ag/$BiVO_4$, and Ag/AgCl/$BiVO_4$ were measured from reflectance values as 3.4, 2.41, 1.75, and 2.4 eV. The surface plasmonic resonance effect of Ag was seen clearly, that reduced the band gap energy from 2.41 eV to 1.75 eV [43].

2.2. Experimental Set-up

The photocatalytic degradation of CBZ over prepared Ag/AgCl/$BiVO_4$ was conducted in a jacketed 200 mL glass reactor equipped with a thermometer and sampling injector. The reaction mixture was stirred continuously with magnetic stirrer (IKA C-MAG HS 7) continuously. Two block LED lamps (Cem Dağ Lighting, LED Icon CL5515) were used as a light source. Each block has 16 LED lamps with total power of 93.4 W. The peak and dominant wavelengths of the LED lamps are 445 nm and 531.5 nm, respectively. The glass reactor was placed between two block LED lamps and the distance between the light source and solution surface was 15 cm, see Fig. 2a.

For a typical procedure in the runs, 200 mL of CBZ aqueous solution with known concentration was prepared from 20 ppm, 1 L of stock solution of CBZ (stored at 0–4 °C) and poured into the reactor. The temperature of reactor was adjusted to 25 °C (for kinetic study, adjusted also to 30, 35 and 40 °C). After reaching the desired temperature, sample was taken thanks to sampling injector and also, pH of reaction was recorded. In the parametric study, pH was adjusted with 0.0025 M of H_2SO_4 (for acidic conditions) and 0.05 M of NaOH (for basic conditions). Then, certain amount of photocatalyst (0.5–1.5 g/L) was added. The suspension was stirred for 30 min in the dark to reach adsorption–desorption equilibrium. However, CBZ concentration before the adsorption was taken as initial concentration. At the end of 4 h of reaction, pH was recorded again. The samples taken at regular intervals were centrifuged and filtered with PTFE (0.45 μm) filter (ISOLAB). The samples were analyzed to determine concentrations of CBZ with High Performance Liquid Chromatography (HPLC) (Agilent 1200) at conditions given in Ref. [43].

In sono-photocatalytic oxidation, low frequency (20 kHz) ultrasonic

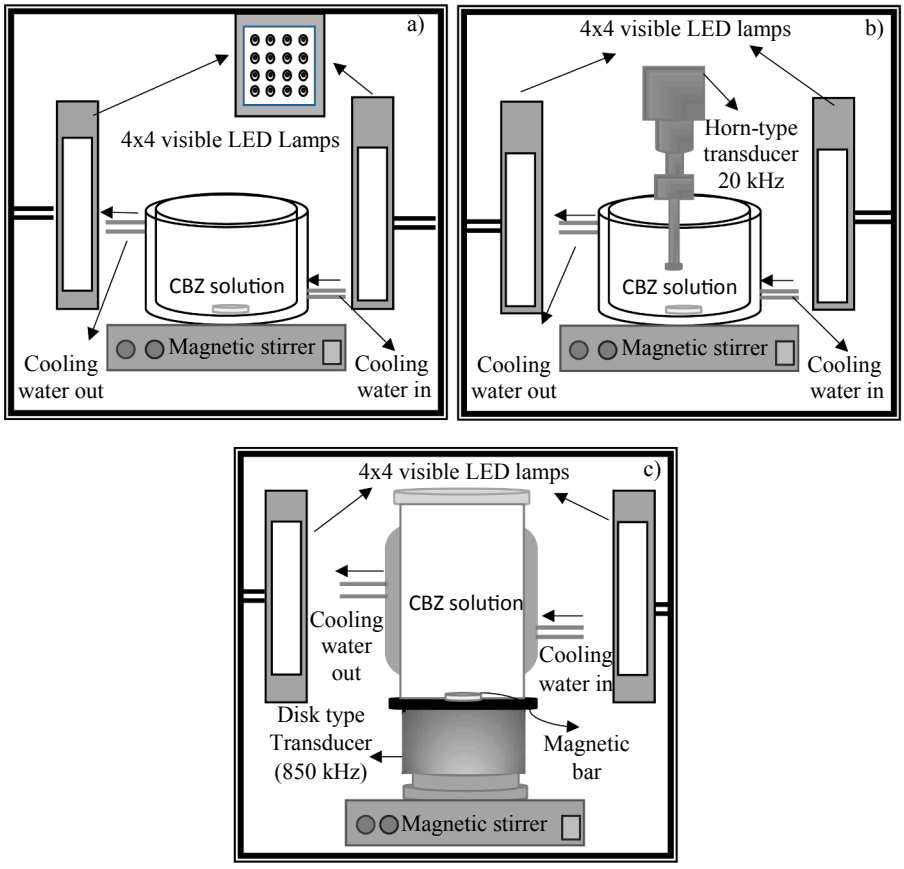

Fig. 2. Experimental Set-up, a) photocatalytic oxidation, b) sono-photocatalytic oxidation with ultrasonic probe system, and c) sono-photocatalytic oxidation with high frequency ultrasonic reactor.

probe system and high frequency (850 kHz) ultrasonic reactor were used as sources of sonication. The output power of probe system (Bandelin HD 3200) was 200 W. The runs were performed in a 200 mL of cooling water jacketed batch reactor. The temperature was kept constant via cooling water circulating around the reactor. The height of the tip of the probe from the bottom of the reactor was kept constant (≈2 cm) for all runs. The experimental setup was placed in a wooden box in order to block the noise from ultrasonic system and to prevent the reaction mixture from being affected by sunlight, see Fig. 2b.

Ultrasonic reactor (Meinhardt E/850/T) at a frequency of 850 kHz and output power of 100 W was used as a high frequency ultrasonic source. Continuous mode and pulse mode of 1:5, and 5:1 were tested in the runs. Cooling water jacketed glass reactor was placed in a closed box to bock the sunlight reach to the reaction solution, see Fig. 2c.

The actual power dissipated into the system was measured by calorimetry (mentioned in part 2.3) for both sonication sources.

2.3. Efficiency of sonication

The acoustic efficiency was calculated using calorimetric method owing to the increase of temperature in a volume of 200 mL of water via Eq. 1. The increase in temperature per unit of sonication time (K s^{-1}) was recorded every 5 s during the sonolysis process of 180 s. In the sonication, ultrasonic power can either be expressed as ultrasonic intensity (related to the transmitted area of ultrasound) or be expressed as power density (related to the solution volume). In the presented study the term of power density was used, Eq. (2) [13,44].

$$Power = (dT/dt)c_pM \quad (1)$$

where c_p = heat capacity of water (4.187 kJ $kg^{-1}K^{-1}$ at 20 °C) and M = mass of water used.

The power density dissipated into the system is given by equation (2)

$$Power\ density = power/volume\ of\ solution \quad (2)$$

Table 1 presents the ultrasonic power densities for each ultrasonic system determined by calorimetry.

3. Results and discussion

3.1. Parametric study in photocatalytic oxidation of CBZ over Ag/AgCl/$BiVO_4$

In the parametric study over Ag/AgCl/$BiVO_4$, the effects of pH, catalyst loading (g/L) and initial CBZ concentration (ppm) on photocatalytic oxidation of CBZ were investigated. In order to optimize these conditions of photocatalytic oxidation, the response surface methodology was used in the Central Composite Design (CCD) of experiments.

For three variables (n = 3) which are pH (X_1), catalyst loading (g/L) (X_2) and initial CBZ concentration (ppm) (X_3) (represented in Table 2), the central composite design can be represented by points on a cube. In the cube, each axis correspond to a factor and central composite design

Table 1
Power densities of low frequency (20 kHz) and high frequency (850 kHz) systems.

Equipment	US amplitude (%)	US Mode	Volume (mL)	Power density (W/mL)
20 kHz Probe	20%	continuous	200	0.15
	30%	continuous	200	0.23
	40%	continuous	200	0.30
850 kHz Reactor	25%	continuous	200	0.02
	50%	continuous	200	0.03
	75%	continuous	200	0.12
850 kHz Reactor	75%	Pulse (1:5)	200	0.014
	75%	Pulse (5:1)	200	0.029

Table 2
Independent variables and their levels in photocatalytic oxidation of CBZ

Variables						
Un-coded	Coded	Levels				
		−0.5	−1	0	1	0.5
pH	X_1	5.5	4	7	10	8.5
Catalyst Loading, g/L	X_2	0.75	0.5	1	1.5	1.25
Initial CBZ Concentration, ppm	X_3	7.5	5	10	15	12.5

is consists of 20 experiments, including 2^n ($2^3 = 8$) factor points, 2^n ($2 \times 3 = 6$) axial points and 6 center points (six replications). Experiments were performed according to experimental plan which is given in Table 3.

The mathematical correlation between pH, catalyst loading (g/L) and initial CBZ concentration (ppm) was developed by a nonlinear polynomial model including 3 squared terms, 3 two factor interaction terms, 3 linear terms to give one response variable, Y as shown in Eq. (3):

$$Y = \beta_0 + \sum \beta_i X_i + \sum \beta_{ii} X_i^2 + \sum \beta_{ij} X_i X_j \quad (3)$$

Where, Y is the predicted degradation (%) response, β_0 is the value of the fitted responses at the central point of the experiment (offset term); β_i, β_{ii}, β_{ij} are the linear, squared and the interaction-regression coefficients of the model, respectively. $X_i and X_j$ are the coded variables.

The experimental values of CBZ degradation under different experimental conditions are given in Table 3. The significance of the parameters on the photocatalytic oxidation of CBZ were determined using Analysis of Variance (ANOVA) with a confidence level of 95% (Minitab-18 software, Student version).

By analyzing the experimental results through CCD, an empirical correlation for the best photodegradation was found to be (Eq. 4):

$$Y = 95.3 + 5.97X_1 - 30.9X_2 - 1.87X_3 - 0.420X_1{*}X_1 + 13.9X_2{*}X_2 - 0.198X_3{*}X_3 - 0.354X_1{*}X_2 + 0.1321X_1{*}X_3 + 2.117X_2{*}X_3 \quad (4)$$

Where X_1 = pH, X_2 = Catalyst Loading (g/L), X_3 = Initial CBZ concentration (ppm) and Y = Degradation (%)

According to results of runs in Tables 2 and 3, ANOVA results with various data such as degrees of freedom, sum of squares, mean square, F and p values are given in Table 4. Effects of linear terms, squared terms and two factor interaction were also investigated. The significance of each term was evaluated on F-values and p-values. In general, the larger the magnitude of F and smaller the value of p (<0.05), the more significant is the corresponding coefficient term [45–48].

ANOVA analysis shows high R^2 value of 0.9769 with lack of fit value of 0.051. The measured p value of model was very small ($5.3{*}10^{-7}$). These results show that model was well fitted to experimental data. As seen in Table 4, linear terms of pH, catalyst loading and initial CBZ concentration have significant effect on degradation of CBZ with p values of 0.00413790, 0.00000377 and 0.00000002, respectively, which were smaller than 0.05. In addition, interaction between pH and initial CBZ concentration (p = 0.04935007) and interaction between catalyst loading and initial CBZ concentration (p = 0.00013729) were also important, and influenced the photocatalytic degradation of CBZ significantly.

Figure 3 exhibits the interaction plot of pH, catalyst loading and initial CBZ concentration. In Fig. 3, pH, catalyst loading and initial CBZ concentration were labeled as X_1, X_2 and X_3, respectively.

Figure 4 shows the surface plot of degradation % vs pH, catalyst loading at constant 10 ppm of initial CBZ concentration (a), degradation (%) vs pH, initial CBZ concentration at constant 1 g/L of catalyst loading (b), and degradation (%) vs catalyst loading, initial CBZ concentration at constant pH = 7 (c).

In general pH in drinking water, surface water or wastewater ranges

Table 3
Central composite design of the photocatalytic oxidation of CBZ for three independent variables.

Run	X_1	X_2	X_3	pH	Catalyst Loading, g/L	Initial CBZ Concentration, ppm	Degradation, (%)
1	−1	1	1	4.0	1.50	15.0	78.04
2	0	0	0	7.0	1.00	10.0	89.28
3	0	0	−0.5	7.0	1.00	7.5	94.93
4	0	0	0	7.0	1.00	10.0	89.30
5	0	0	0.5	7.0	100	12.5	76.71
6	−0.5	0	0	5.5	1.00	10.0	83.80
7	0.5	0	0	8.5	1.00	10.0	88.43
8	0	0	0	7.0	1.00	10.0	93.20
9	−1	1	−1	4.0	1.50	5.0	100.00
10	−1	−1	1	4.0	0.50	15.0	51.97
11	1	1	−1	10.0	1.50	5.0	100.00
12	0	0	0	7.0	1.00	10.0	90.30
13	1	−1	−1	10.0	0.50	5.0	97.22
14	0	0	0	7.0	1.00	10.0	90.85
15	1	−1	1	10.0	0.50	15.0	62..2
16	0	0	0	7.0	1.00	10.0	90.99
17	0	0.5	0	7.0	1.25	10.0	92.08
18	0	−0.5	0	7.0	0.75	10.0	83.78
19	1	1	1	10.0	1.50	15.0	88.26
20	−1	−1		4.0	0.50	5.0	92.80

Table 4
ANOVA of the response for photocatalytic oxidation of CBZ

Terms	Degrees of Freedom	Sum of Squares	Mean Square	F Value	p Value
Model	9	2652.21	294.69	46.91	0.00000053
pH, X_1	1	85.80	85.80	13.66	0.00413790
Catalyst Loading, X_2	1	519.33	519.33	82.67	0.00000377
Initial CBZ concentration, X_3	1	1661.52	1661.52	264.50	0.00000002
X_1*X_1	1	2.67	2.67	0.42	0.52927557
X_2*X_2	1	2.26	2.26	0.36	0.56209383
X_3*X_3	1	4.59	4.59	0.73	0.41251102
X_1*X_2	1	2.26	2.26	0.36	0.56216319
X_1*X_3	1	31.40	31.40	5.00	0.04935007
X_2*X_3	1	223.98	223.98	35.66	0.00013729
Error	10	62.82	6.28		
Lack-of-Fit	5	52.34	10.47	4.99	0.05108539
Pure Error	5	10.48	2.10		
Total	19	2715.02			
R^2		0.9769			

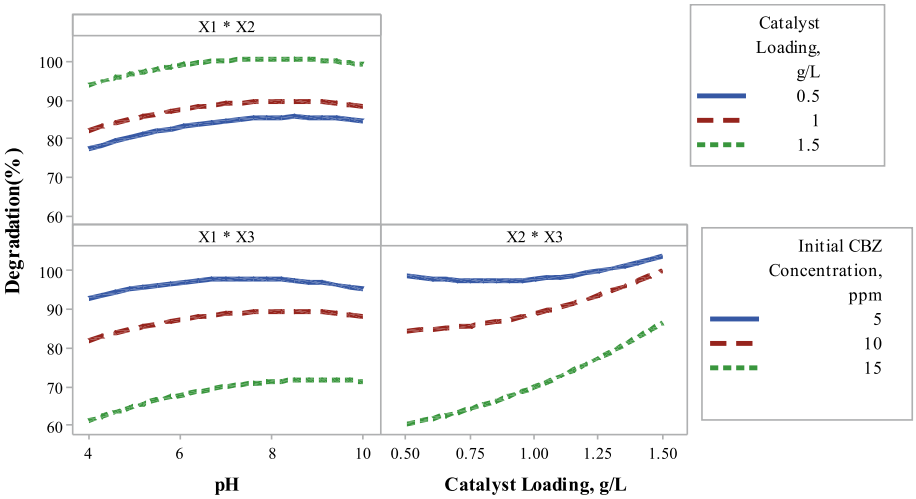

Fig. 3. Interaction plot for degradation % of CBZ.

from 6 to 9 and also, most industrial wastewater pH is neutral or alkaline. Therefore, exploring the effect of pH (X_1) on photocatalytic oxidation is important [49,50]. In this study, pH was selected in range of 4–10. CBZ was found as a molecular state in that pH range because of its pKa values were $pKa_1 = 2.3$ and $pKa_2 = 13.9$. Thus, changes in the initial pH had less effect (p value = $4.1*10^{-3}$) on degradation of CBZ than that initial CBZ concentration (p value = $2*10^{-8}$) and catalyst loading (p value = $3.77*10^{-6}$) [49,51,52].

As seen in Figs. 3 and 4a, in all catalyst loading of 0.5, 1 and 1.5 g/L, increment in initial pH increased the photocatalytic degradation of CBZ.

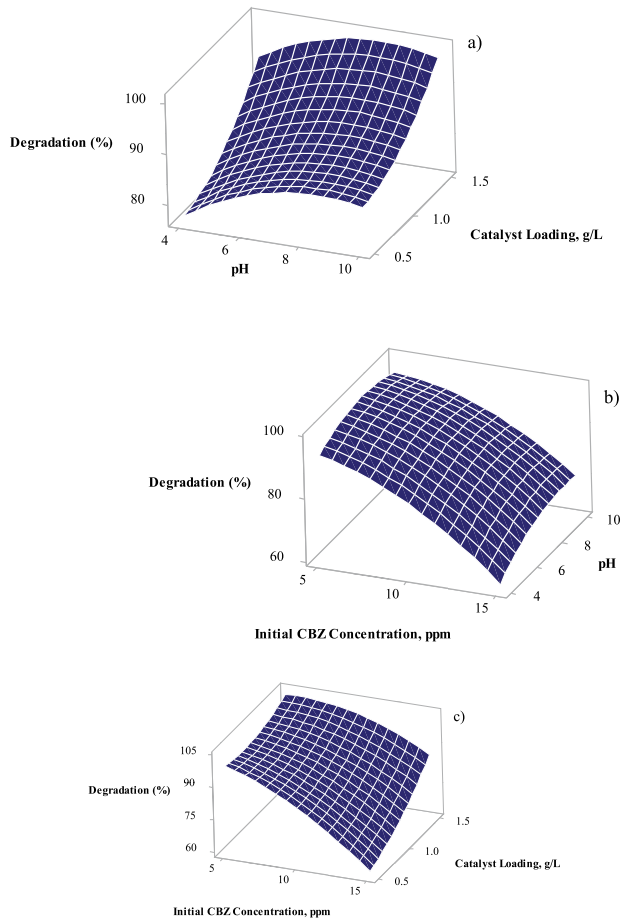

Fig. 4. Surface plots of: a) degradation (%) vs pH, catalyst loading, b) degradation (%) vs pH, initial CBZ concentration, and c) degradation (%) vs catalyst loading, initial CBZ concentration.

This increment is significant up to pH 8.5. After this pH, there was no significant change in degradation with pH of CBZ solution. As can be seen from Table 3, the obtained CBZ degradations were 83.8%, 90.3% (average value) and 88.4% at pH values of 5.5, 7 and 8.5, respectively at the initial CBZ concentration of 10 ppm with catalyst loading of 1 g/L. However, the CBZ degradation was 51.97% at pH 4, catalyst loading of 0.5 g/L at 15 ppm initial CBZ concentration. Increasing pH value to 10 increased the CBZ degradation to 62.02% at the same catalyst loading and initial CBZ concentration. Similarly, at pH = 4, catalyst loading of 1.5 g/L and 15 ppm initial CBZ concentration, the obtained CBZ degradation was 78.04%. Increasing pH to 10 (keeping the initial CBZ concentration and catalyst loading constant) caused an increase in CBZ degradation (88.26%). At low initial concentration of CBZ of 5 ppm, at catalyst loading of 0.5 g/L, degradation of CBZ increased from 92.8% to 97.22% with increasing pH value from 4 to 10. Increasing in initial pH solution slightly increased degradation of CBZ at initial CBZ concentration of 5 ppm. However, degradation of CBZ increased from 78.04% to 88.26% with increasing pH from 4 to 10 at catalyst loading and initial CBZ concentration of 1.5 g/L and 15 ppm, respectively (Figs. 2 and 3b). Results show that alkaline medium influenced photocatalytic oxidation of CBZ positively because in alkaline conditions, photogenerated h^+ in VB of $BiVO_4$ could effectively oxidize OH^- which is produced in alkaline conditions to generate OH• which was more oxidative than that of h^+ [51 –53]. More active role of OH• radicals than that of h^+ in photocatalytic activity was proved in previous study [43].

In order to investigate effect of catalyst loading (g/L) (X_2) on photocatalytic degradation of CBZ, catalyst loading increased from 0.5 g/L to 1.5 g/L. In Figs. 3 and 4a, effect of catalyst loading on degradation in different initial pH values were given. Increase in catalyst loading increased the photocatalytic degradation of CBZ at all pH values. At acidic pH of 4 with 15 ppm initial CBZ concentration, CBZ degradation increased from 51.97% to 78.04% with increasing catalyst loading from 0.5 to 1.5 g/L. At neutral pH of 7 with 10 ppm initial CBZ concentration, CBZ degradation increased from 83.78% to 92.08% with increasing catalyst loading from 0.75 to 1.25 g/L. Similarly, at alkaline condition of pH 10, CBZ degradation increased from 62.02% to 88.26% with increasing catalyst loading from 0.5 to 1.5 g/L while initial CBZ concentration was kept at 15 ppm. Figs. 3 and 4c show that catalyst loading increased the degradation of CBZ in each initial CBZ concentration (5–10–15 ppm). However, effect of catalyst loading is higher at high initial CBZ concentration (15 ppm) than that of low initial concentrations of CBZ (5 and 10 ppm). Because, low catalyst loading has enough surface area and active sites for low CBZ concentration. For instance, in the presence of 5 ppm CBZ, when catalyst loading was increased from 0.5 to 1.5 g/L, degradation of CBZ changed slightly from 97.22% to 100% at pH 10, respectively. However, when initial CBZ concentration was increased, more catalyst loading was required and in the case of the presence of 15 ppm of CBZ, degradation of CBZ increased from 62.02% to 88.26% with increase in catalyst loading from 0.5 g/L to 1.5 g/L at pH 10, respectively. Thus, high impact of catalyst loading could be seen in higher initial CBZ concentration. In general, more catalyst addition enhance the photocatalytic oxidation, because, increase in the catalyst loading causes increasing the number of active sites on the photocatalyst surface, and speed up the formation rate of active species that oxidizes the organic pollutants [49,54,55].

The effect of initial CBZ concentration (X_3) was also investigated with various CBZ concentrations which were selected as 5, 10 and 15 ppm. As seen in Table 3, CBZ degradation decreased from 94.93% to 90.32% and then to 76.71% with increasing initial CBZ concentration from 7.5 ppm to 10 ppm and then to 12.5 ppm at a catalyst loading of 1 g/L and pH 7. Similar decrease was obtained at pH 4 at a catalyst loading of 1.5 g/L. In that condition, CBZ degradation decreased from 100% to 78.04% with increasing initial CBZ concentration from 5 to 15 ppm. Similarly, the obtained degradation was 97.22% at pH 10, a catalyst loading of 0.5 g/L with 5 ppm initial CBZ concentration, however degradation was decreased to 62.02 % with increasing initial CBZ concentration to 15 ppm. As seen in Fig. 3 and 4b-c, when initial concentration of CBZ was increased, degradation efficiency decreased at each pH or each catalyst loading. Decline in degradation with increasing initial CBZ concentration may be explained by the increase in initial CBZ concentration is required more surface area of catalyst and active sites. A certain amount of catalyst can degrade certain amount of CBZ. Besides, increase in initial CBZ concentration may retard penetration of light photons to the catalyst surface that cause in decrease in photocatalytic efficiency [28,56–58].

Figure 5 represents the experimental (actual) and predicted degradation values (obtained from CCD analysis) in photocatalytic degradation of CBZ (Table 3). As seen, between the experimental data and predicted degradation values, there is a good correlation. This showed that the experimental data fits well with the model in the range studied.

Figure 6 represents the example HPLC chromatogram for degradation of CBZ under following experimental conditions: $[CBZ]_0 = 10$ ppm, Catalyst loading = 1 g/L, T = 298 K, pH = 7, and LED light power = 93.4 W, continuous stirring of 200 rpm).

The decrease in CBZ concentration with oxidation is very clear (the HPLC peak at the retention time of 5.1 min). The HPLC peaks at 2.5 min, 3.0 min and 3.8 min retention times presents the intermediates occurred at the end of photocatalytic oxidation of CBZ. The shorter residence times of formed intermediates means that the formed intermediates are more hydrophilic than that of CBZ molecule. In the photocatalytic oxidation of CBZ, pH of the solution was measured at the beginning and at the end of reaction of 4 h. At the beginning of reaction the pH of the solution was adjusted to 7.0 and it decreased to 3.0 at the end of 4 h of

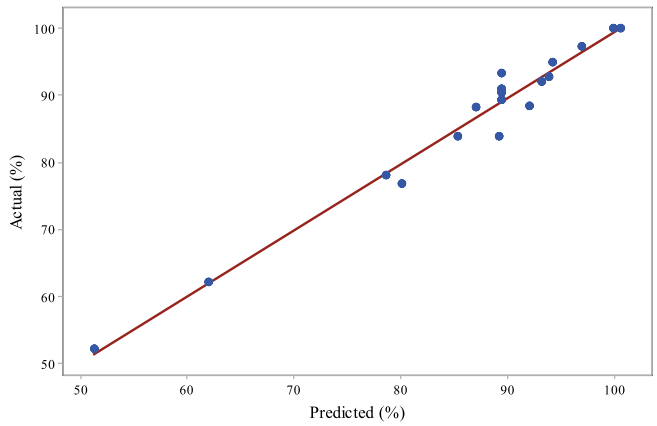

Fig. 5. Actual (experimental) vs. predicted degradation values for photocatalytic oxidation of CBZ.

reaction. The decrement in pH also shows the formation of acidic intermediates during the photocatalytic reaction.

Table 5 shows predicted degradation values (%) and obtained TOC reductions (%) in photocatalytic oxidation of CBZ over Ag/AgCl/$BiVO_4$ for each runs.

As seen from Table 5, in each run, the obtained TOC reductions were less than degradation percentages of CBZ. This result was also a good evidence of degradation of CBZ into oxidation-resistant intermediates rather than CO_2 and water. At acidic pH of 4.0, the TOC reductions (between 0 and 1.94%) were lower than that at pH = 7.0 (between 3.58 and 6.72%) and at pH = 10.0 (between 7.95 and 14.04%), Table 5.

3.2. Kinetic study

The effect of temperature on photocatalytic oxidation of CBZ was investigated over Ag/AgCl/$BiVO_4$ photocatalyst under visible LED light irradiation under following conditions: $[CBZ]_0$ = 10 ppm, 200 mL, catalyst loading = 1 g/L, without pH regulation at various temperatures of 25 °C (298 K), 30 °C (303 K), 35 °C (308 K) or 40 °C (313 K).

Figure 7a shows degradation percentages of CBZ over Ag/AgCl/$BiVO_4$ photocatalyst under mentioned conditions above.

Figure 7b exhibits TOC reductions and degradation percentages of CBZ over Ag/AgCl/$BiVO_4$ photocatalyst after a reaction time of 240 min at 298 K, 303 K, 308 K, 313 K.

As seen in Fig. 7a, degradation of CBZ was increased slightly with raise in reaction temperature up to 308 K. At 298 K, degradation was 90.3%. When temperature increased to 303 K, degradation of CBZ increased slightly to 91.76%. Degradation of CBZ was achieved as 93.37% at 308 K. However, degradation of CBZ decreased slightly to

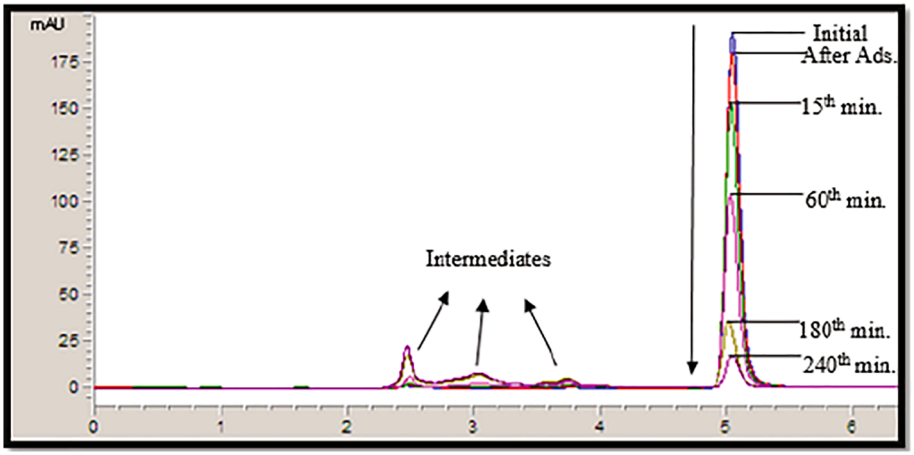

Fig. 6. HPLC chromatography analysis.

Table 5
Predicted degradation values (%) and obtained TOC reductions (%) in photocatalytic oxidation of CBZ for three independent variables

pH	Catalyst Loading, g/L	Initial CBZ Concentration, ppm	Degradation, (%)	Predicted Degradation (%)	TOC reduction(%)
4.0	1.50	15.0	78.04	78.622	1.94
7.0	1.00	10.0	89.28	89.446	6.72
7.0	1.00	7.5	94.93	94.130	6.29
7.0	1.00	10.0	89.30	89.446	3.58
7.0	1.00	12.5	76.71	80.087	3.7
5.5	1.00	10.0	83.80	89.157	4.53
8.5	1.00	10.0	88.43	92.011	7.26
7.0	1.00	10.0	93.20	89.446	5.31
4.0	1.50	5.0	100.00	99.868	1.55
4.0	0.50	15.0	51.97	51.247	0
10.0	1.50	5.0	100.00	100.561	14.04
7.0	1.00	10.0	90.30	89.446	5.02
10.0	0.50	5.0	97.22	96.896	7.95
7.0	1.00	10.0	90.85	89.446	5.54
10.0	0.50	15.0	62.02	61.970	8.55
7.0	1.00	10.0	90.99	89.446	4.88
7.0	1.25	10.0	92.08	93.104	6.21
7.0	0.75	10.0	83.78	85.344	2.29
10.0	1.50	15.0	88.26	87.020	10.78
4.0	0.50	5.0	92.80	93.878	0

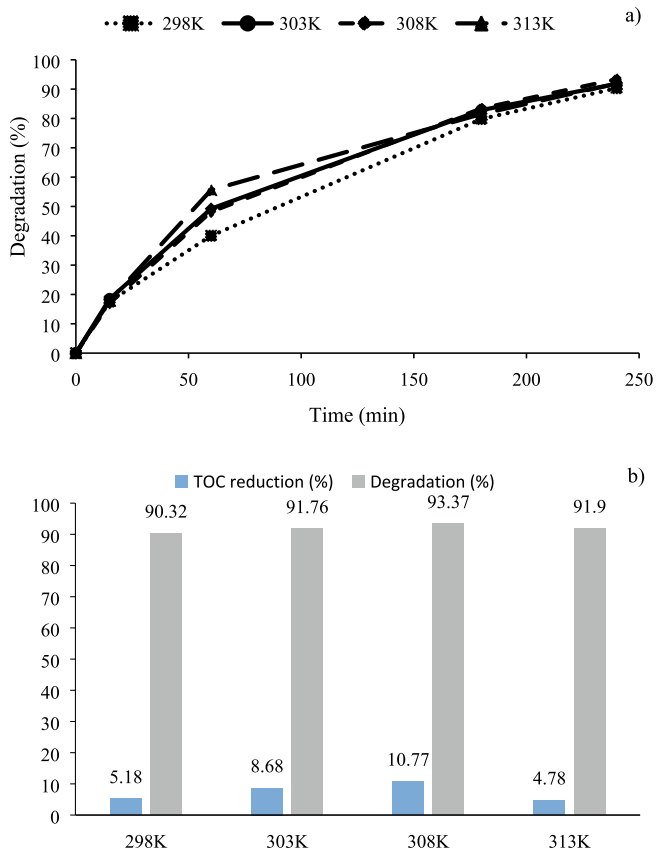

Fig. 7. Effect of temperature on a) photocatalytic oxidation of CBZ over Ag/AgCl/$BiVO_4$ photocatalyst b) TOC reductions and CBZ degradation after 240 min of reaction ($[CBZ]_0$: 10 ppm, Catalyst loading = 1 g/L, T = 298 K, 303 K, 308 K, 313 K, without pH regulation, and LED light power = 93.4 W, continuous stirring of 200 rpm).

91.9% at 313 K. It is known that temperature has little effect on photocatalytic oxidation [59], the same as in this study. The photocatalytic reactions are usually not very temperature sensitive, because the band gap energy of the semiconductive catalysts is too high (for $TiO_2 \approx 3.0$ eV, for Ag/AgCl/$BiVO_4$ photocatalyst used in this study = 2.4 eV) to be overcome by the thermal activation energy (kT ≈ 0.026 eV at room temperature) [60]. The small increase in degradation with increasing temperature can be explained by the increase in rate constant of photocatalytic oxidation. So, the degradation of CBZ increased in the temperature range of 298 K – 308 K. The obtained lower degradation degree with further increasing temperature to 313 K may be explained by the limitation of adsorption of CBZ on Ag/AgCl/$BiVO_4$ photocatalyst to react with active radicals for oxidation [61,62]. To confirm this result, adsorption experiments were conducted in the dark. After the 30 min dark adsorption experiment, 1.69% of adsorption of CBZ was measured at a temperature of 298 K, however 0.2 % of adsorption of CBZ was measured at 313 K. In addition to this, dissolved O_2, which is one of the major parameters, was disappeared from the system at higher temperatures [63]. As mentioned in previous study [43], $O\bullet_2^-$ radicals are the major free radicals that improve photocatalytic oxidation of CBZ. Production of $O\bullet_2^-$ radicals is possible if proper amount of dissolved O_2 react with conduction band electrons (e_{CB}^-). Thus, the optimum temperature was selected as 308 K in photocatalytic oxidation of CBZ over Ag/AgCl/$BiVO_4$ photocatalyst.

Temperature rise up to 308 K influenced TOC reduction positively and TOC reductions were found as 5.18%, 8.86% and 10.77% at 298 K, 303 K and 308 K, respectively. When temperature raised to 313 K, TOC reduction of CBZ decreased from 10.77% to 4.78% after a reaction time 240 min, exactly as obtained in CBZ degradation results (Fig. 7b).

Very few studies are available in literature which investigated the effect of temperature on photocatalytic oxidation of pollutants. The effect of temperature on aniline photodegradation in aqueous solution in the presence of TiO_2 and UV was investigated by Shahrezaei et al. (2012) [64] in the range of 293–323 K. Increase in temperature from 293 to 323 K reduced the time required for aniline removal. However, in the study done by Soares et al. (2007) [61] photoactivated degradation reaction of Rhodamine B (RB) was studied using P-25 TiO_2 (Degussa) as catalyst in the temperature range of 293–353 K. The optimum temperature was selected as 313 K. Similarly, Chatzitakis et al. (2008) [60] studied the photocatalytic oxidation of antibiotic drug chloramphenicol over TiO_2-P25 catalyst at the temperature range of 278–330 K. They observed that, by increasing the temperature, an increase of reaction rate constant is achieved until 318 K, while temperatures higher than 318 K lead to a decrease in photocatalytic activity of TiO_2-P25 catalyst.

In literature, photocatalytic oxidation of CBZ over different catalysts mostly obeyed first order kinetics. These are some examples: BiOCl/Fe_3O_4 photocatalyst [51], Ag/AgCl/$Bi_4Ti_3O_{12}$ photocatalyst [20] and graphene quantum dots loaded on $BiVO_4$ photocatalyst [28]. However, in the study done by Gao et al (2019) [65] the photocatalytic degradation kinetic of CBZ over BiOCl photocatalyst was recorded as a function of irradiation time and the data were fitted to a second-order rate model. So, to investigate the photocatalytic oxidation kinetics of CBZ over Ag/AgCl/$BiVO_4$ photocatalyst, first and second order kinetics were investigated in this study.

First (Eq. (5)) and second order (Eq. (7)) reaction kinetics were tested by using Eqs. (6) and (8) for photocatalytic oxidation of CBZ over Ag/AgCl/$BiVO_4$ photocatalyst and the calculated reaction rate constants are given in Table 6 with the regression coefficients.

For first order kinetics:

$$-r_{CBZ} = -\frac{dC_{CBZ}}{dt} = k_1 * C_{CBZ} \quad (5)$$

$$-\ln * \frac{C_{CBZ}}{C_{CBZ_0}} = k_1 * t \text{ and}$$

$$-\ln(1-x) = k_1 * t \quad (6)$$

For second order kinetics:

$$-r_{CBZ} = -\frac{dC_{CBZ}}{dt} = k_2 * {C_{CBZ}}^2 \quad (7)$$

$$\frac{1}{C_{CBZ}} - \frac{1}{C_{CBZ_0}} = k_2 * t \text{ and}$$

$$\frac{x}{1-x} = k_2 * C_{CBZ_0} * t \quad (8)$$

Where C_{CBZ} is concentration of CBZ at any time, mol/dm^3, C_{CBZ0} is initial CBZ concentration, mol/dm^3, t is sampling time as minutes, x is CBZ degradation degree, and k_1 and k_2 are first and second order reaction rate constants, respectively.

In Table 6, first and second order reaction rate constants in photocatalytic oxidation of CBZ were given with regression coefficients at the corresponding temperatures. As seen in Table 6, regression coefficients of first order reaction kinetics were found as higher than that of second

Table 6
First and second order reaction rate constants in photocatalytic oxidation of CBZ, regression coefficients at different temperatures

	First Order		Second Order	
Temperature, K	Reaction Rate Constant, k_1 (min^{-1})	Regression Coefficient, R^2	Reaction Rate Constant, k_2 (dm^3/mol*min)	Regression Coefficient, R^2
298	0.0094	0.995	753.7	0.879
303	0.0102	0.997	907.3	0.889
308	0.0108	0.993	1093.9	0.836
313	0.0102	0.985	904.9	0.867

order at each temperature. According to higher regression coefficients of first order kinetics than that of second order kinetics, it can be said that photocatalytic oxidation of CBZ follows first order kinetics under studied experimental conditions.

Figure 8 shows first order kinetic model of photocatalytic oxidation of CBZ over Ag/AgCl/$BiVO_4$ photocatalyst under mentioned conditions above. As given in Fig. 8 and Table 6, reaction rate constants were found as 0.0094, 0.0102, 0.0108 and 0.0102 min^{-1} at 298, 303, 308 and 313 K, respectively. First order reaction rate constants increased from 0.0094 min^{-1} to 0.0102 min^{-1} and then to 0.0108 min^{-1} with increasing temperature from 298 K to 303 K and then to 308 K. Then, the reaction rate constant was decreased to 0.0102 min^{-1} due to the mentioned reason above.

Figure 9 represents graph of lnk versus 1/T for 298, 303 and 308 K. To calculate activation energy, Arrhenius Equation was used (Eqs. 9 and 10). Firstly, lnk and 1/T were calculated and then, graph of lnk versus 1/T was plotted.

$$k = A^{*}e^{-E/(R^{*}T)} \tag{9}$$

$$\ln k = \ln A - \frac{E}{R} * \frac{1}{T} \tag{10}$$

From the slope of Arrhenius plot, $-E/R$, (where R is universal gas constant (8.314 J/mol*K and E is activation energy) Activation Energy, E could be calculated. Intercept of graph of lnk versus 1/T gives the lnA to calculate Arrhenius constant (A).

The Activation energy and Arrhenius constant were calculated as 10.6 kJ/mol and 0.68, respectively. So, the rate of photocatalytic oxidation of CBZ can be written as (Eq. (11)):

$$-r_{CBZ} = 0.68^{*}e^{-\frac{10.6}{RT}*}C_{CBZ} \tag{11}$$

at the experimental conditions tested in this study. To the best of our knowledge, no study so far has measured the activation energy in photocatalytic oxidation of CBZ over any prepared catalysts in literature.

3.3. Effect of sonication on photocatalytic oxidation of CBZ

Sono-photocatalytic degradation process is one of the effective AOPs to degrade a wide range of contaminants in wastewater. Ultrasound (US) with suitable catalysts (sono-catalysis) shows an environmentally friendly property to treat hazardous organic pollutants in wastewater but, the degradation rate is slow when it is compared with other established methods. Combination of US with light irradiation enhances the efficiency of semiconductor-mediated degradation of aqueous pollutants synergistically [66].

In order to investigate the effect of sonolysis on photocatalytic oxidation of CBZ, sonication, photocatalytic oxidation, sono-catalytic and sono-photocatalytic oxidation experiments were carried out over Ag/AgCl/$BiVO_4$ photocatalyst under following conditions: CBZ initial

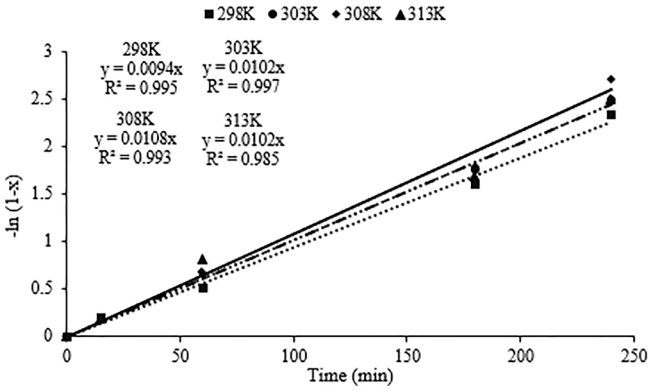

Fig. 8. First order kinetic model of photocatalytic oxidation of CBZ.

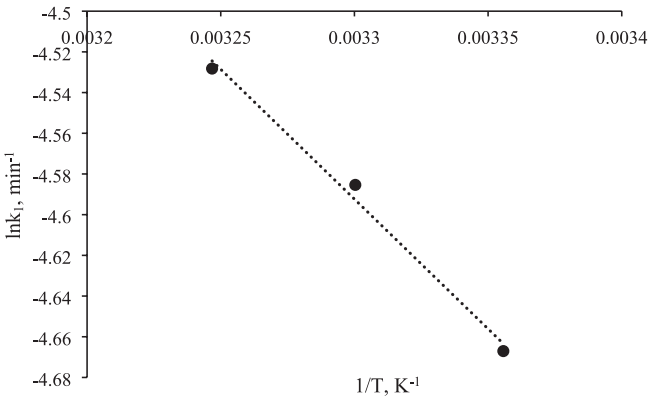

Fig. 9. lnk versus 1/T relationship.

concentration of 10 ppm (42 μM), Temperature = 298 K, without pH regulation, catalyst loading = 1 g/L, volume of the CBZ solution = 200 mL, and under continuous stirring of 200 rpm. In the runs of sonication, ultrasonic probe (Bandelin, UW3200) which has a frequency of 20 kHz and high frequency ultrasonic reactor (850 kHz, Meinhardt Ultraschalltechnik) were used as sources of sonication. In the catalytic experiments, adsorption–desorption equilibrium was achieved in the dark for 30 min. After 30 min of adsorption–desorption equilibrium, LED lights and/or sonication were turned on and experiments were started for photocatalytic and sono-photocatalytic oxidation of CBZ. The reaction duration was 60 min in these runs. Experiments were repeated at least two times mostly three times. The standard deviation of the average of the independent runs changed in the range of ± 0.10 and ± 3.8. The average values were used in the Figures with error bars.

Figure 10 shows the degradation of CBZ by sonication, photocatalytic oxidation, sono-catalytic and sono-photocatalytic oxidation using the low frequency ultrasonic probe (20 kHz) (a) and high frequency ultrasonic reactor (b) as sources of sonication.

In low frequency sonication system (20 kHz), sonication and sono-catalytic oxidation were achieved CBZ degradation of 27.12 and 28.05%, respectively. On the other hand, photocatalytic oxidation of CBZ was 44% at the end of 60 min of reaction time. As seen in Fig. 10a, sonication enhanced the photocatalytic oxidation of CBZ and increased the degradation percentage from 44% to 65.42% after 60 min of reaction time, Fig. 10a.

TOC reductions were not achieved in sonication and sono-catalytic oxidation. In photocatalytic oxidation, TOC reduction was 0.52% at the end of 60 min of reaction time. The highest TOC reduction was obtained as 6% in sono-photocatalytic oxidation. Positive effect of sonication was observed for TOC reduction of CBZ.

Synergistic effect between photocatalytic oxidation and sono-catalytic oxidation was investigated at low frequency (20 kHz). To examine the synergistic effect, kinetic results of photocatalytic, sono-catalytic and sono-photocatalytic oxidations in terms of first order rate constants were calculated. Synergistic effect in experiments with low frequency (20 kHz) can be observed when reaction rate constant of sono-photocatalytic oxidation ($k_{Vis+US+Catalyst}$) is higher than the sum of reaction rate constants of sono-catalytic ($k_{US+Catalyst}$) and photocatalytic oxidation ($k_{Vis+Catalyst}$) (Eq. (12)) [8,32].

$$k_{Vis+US+Catalyst} > (k_{Vis+Catalyst} + k_{US+Catalyst}) \tag{12}$$

Reaction rate constants for sono-catalytic oxidation ($k_{US+Catalyst}$) and photocatalytic oxidation ($k_{Vis+Catalyst}$) were found as 0.0058 and 0.0094 min^{-1}, respectively. As seen from Eq. 13, the sum of two reaction rate constants of sono-catalytic oxidation ($k_{US+Catalyst}$) and photocatalytic oxidation ($k_{Vis+Catalyst}$) was 0.0152 min^{-1} which was lower than reaction rate constant of sono-photocatalytic oxidation ($k_{Vis+US+Catalyst}$) as 0.0187 min^{-1}. The result shows that 18.7% of synergistic effect was

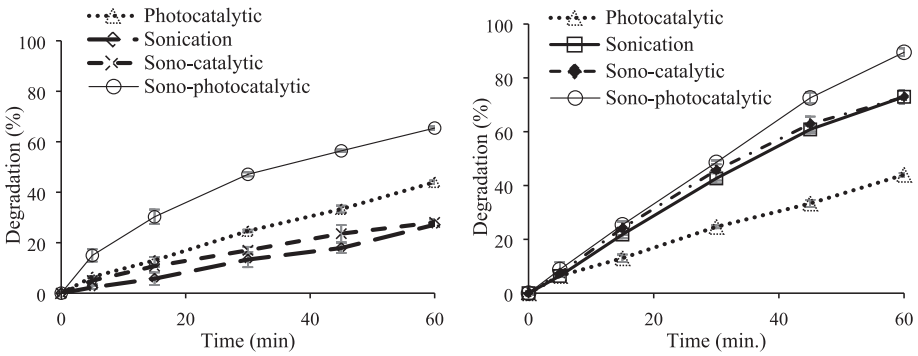

Fig. 10. Effect of sonolysis on photocatalytic oxidation of CBZ a) using low frequency (20 kHz) US at 0.15 W/mL b) using high frequency (850 kHz) ultrasonic bath at 0.12 W/mL ($[CBZ]_0$ = 10 ppm, Catalyst loading = 1 g/L, T = 298 K, without pH regulation, and LED light power = 93.4 W, continuous stirring of 200 rpm).

observed between sono-catalytic oxidation and photocatalytic oxidation.

$$0.0187 min^{-1} > 0.0094 min^{-1} + 0.0058 min^{-1} \quad (13)$$

In the high frequency sonication system (850 kHz), sonication alone achieved 72.97% of CBZ degradation after a reaction time of 60 min. Catalyst addition to sonication (sono-catalytic oxidation) didn't change degradation of CBZ (72.89%). However, the degradation percentage of CBZ reached to 89.5% in sono-photocatalytic oxidation of CBZ after 60 min of reaction at high frequency sonication at a power density of 0.12 W/mL, Fig. 10b.

Synergistic effect between photocatalytic oxidation and sono-catalytic oxidation was also investigated at high frequency (850 kHz) ultrasonic reactor at a power density of 0.12 W/mL. Kinetic results of photocatalytic ($k_{Vis+Catalyst}$), sono-catalytic ($k_{US+Catalyst}$) and sono-photocatalytic ($k_{Vis+US+Catalyst}$) oxidations in terms of first order rate constants were calculated as 0.0094, 0.0215 and 0.0322, min^{-1}, respectively. Synergistic effect caused the reaction rate constant of sono-photocatalytic oxidation ($k_{Vis+US+Catalyst}$) to be higher than the sum of reaction rate constants of individual sono-catalytic ($k_{US+Catalyst}$) and photocatalytic oxidation ($k_{Vis+Catalyst}$), Eqs. (14), 15 [8,32].

$$k_{Vis+US+Catalyst} > (k_{Vis+Catalyst} + k_{US+Catalyst}) \quad (14)$$

$$0.0322 min^{-1} > 0.0094 min^{-1} + 0.0215 min^{-1} \quad (15)$$

A synergetic effect of 4.04 % was measured between sono-catalytic oxidation and photocatalytic oxidation in the high frequency (850 kHz) ultrasonic reactor system at a power density of 0.12 W/mL.

The frequency is the very important parameter in the sonochemical oxidation process. As seen from Fig. 10a and b, high frequency sonication was more effective for degradation of CBZ, 27.12 % and 72.97 % CBZ degradation was achieved in low and high frequency ultrasonic system, respectively. Degradation of 65.42 % and 89.5 % were achieved in sono-photocatalytic oxidation of CBZ at low (20 kHz) and high (850 kHz) frequency ultrasonic system at power densities of 0.15 and 0.12 W/mL, respectively. At high frequencies, due to the fast cavitation events per unit time, short life-time and small cavitation bubbles form. Although these small cavitation bubbles collapse less violently, more cavitation events cause production of sufficient number of active radicals from water dissociation [67]. As the frequency is increased, the pulsation and collapse of bubble occur more rapidly causing more hydroxyl radicals to escape from the bubble [67]. A greater number of oscillations of cavitation bubbles increases the mass transfer of OH• radicals into the bubble–liquid interface and concurrently increase the diffusion of CBZ molecules from liquid to the bubble. Due to increment of active radicals' number, CBZ degradation increased highly in sono-photocatalytic oxidation of CBZ, and a high degradation of 89.5% was achieved at the end of 60 min of reaction in high frequency ultrasonic system.

It is known that the major physicochemical parameters of organic compounds that might influence the degradation in sonication is partition coefficient, solubility, vapor pressure and Henrys law constant. Mostly, the volatile and hydrophobic compounds degrade in the interior of the cavitation bubble. The cavitation bubble–liquid interface of the bubble is also a high-temperature region. This region is hydrophobic, and the chance of binding hydrophobic substance in this region is probably high, thus the hydrophobic substances can undergo easy degradation in this region. However, hydrophilic substances are found in the liquid phase, and degrade by oxidation with $OH^{\cdot}$ and H_2O_2 which escape from the cavitation bubble–liquid interface. Both low frequency and high frequency sonication systems caused an increase in photocatalytic efficiency [68]. This result was expected, because CBZ has moderate hydrophobic character with partition coefficient (K_{OW}) of 2.45 and solubility of 17.7 mg L^{-1}. As mentioned above, hydrophobic compounds degrade in the cavitation bubble and/or cavitation bubble–liquid interface via pyrolysis due to the high temperature and active radicals that are more abundant in these regions [44].

In literature there are some studies which investigated the effect of frequency on sono-catalytic oxidation of various organic compounds. In the study of Choi et al. [69], TiO_2-incorporated nano-structured carbon (i.e., carbon nanotubes (CNTs) or graphene (GR)) composites were synthesized and tested in sono-catalytic oxidation of Rhodamine B (RhB). Effect of ultrasound frequency was investigated at frequencies of 35, 500 and 1000 kHz under the conditions: $[RhB]_0$ = 10 ppm, Volume of RhB = 500 mL, Catalyst loading = 50 g/L, T = 294 K, and Stirring speed = 120 rpm. The rate constants for removal reaction of the RhB were calculated as 4.2×10^{-3}, 4.7×10^{-3}, and 3.5×10^{-3} min^{-1} at 35, 500, and 1000 kHz for P25 while TiO_2-GR-5 had 9.4×10^{-3}, 14.5×10^{-3}, and 6.4×10^{-3} min^{-1}, respectively. Among these frequencies, 500 kHz was found as optimum frequency due to the highest kinetic constants. Also, Ayanda et al. (2018) investigated effect of frequency of 20, 60 and 100 kHz on the degradation of PSP under following experimental condition: $[PSP]_0$ = 100 ppm, volume of PSP = 100 mL, Stirring speed = 300 rpm. At the end of 60 min of reaction, 60 kHz was found as optimum frequency because degradation of PSP was higher at frequency of 60 kHz (11.71 %) than that of frequency of 20 kHz (2.41 %) and 100 kHz (5.39%) [70]. In the sono-catalytic oxidation of BPA over $LaFeO_3$ perovskite catalyst, 20 kHz and 850 kHz ultrasonic frequency systems were used as source of sonication. It was reported that, the obtained BPA removal (96.8 %) using high frequency (850 kHz) ultrasonic reactor was slightly higher than that obtained using low frequency (20 kHz) ultrasonic probe system (91.5%) at the same power density of 0.091 W/mL, however, higher mineralization (TOC reduction) of BPA was achieved in 850 kHz ultrasonic reactor (37.8 %) than that of the 20 kHz probe system (26.7%) [44].

However, to prove the real effect of the sonication in the present study, the degradation experiments were also conducted in the absence of photocatalyst under visible light (vis), visible light and stirring at

1500 rpm (vis + stirring), visible light and sonication at 20 kHz, 0.15 W/mL without stirring (vis + sonication at 20 kHz), and lastly, visible light and sonication at 850 kHz kHz, 0.12 W/mL without stirring (vis + sonication at 850 kHz). Fig. 11 presents these results.

As seen in Fig. 11, visible LED light irradiation could degrade only 4.22% of CBZ without Ag/AgCl/$BiVO_4$ and sonication, indicating the photodegradation of CBZ under visible LED light irradiation could be ignored. In the case of, degradation of CBZ under visible LED light and stirring at 1500 rpm, negligible degradation was obtained as 4.35%. On the other hand, the degradations of 28.02% and 73.81% were achieved under the visible light and sonication at 20 kHz and 850 kHz, respectively. So it could be said that, the obtained degradations were due to the chemical effect of sonication.

The real effect of sonication was also investigated in the presence of catalyst. In these runs, the results of the photocatalytic oxidation (vis + catalyst) at different stirring of 200, 500 and 1500 rpm were compared with the results of sono-photocatalytic oxidation at the frequencies of 20 and 850 kHz. As seen in Fig. 12, the degradations in the photocatalytic oxidation of CBZ were 44%, 46%, and 50% at the stirring speed of 200, 500 and 1500 rpm. The small increase in degradation may be due to the decreasing of external mass transfer resistance. Whereas, the degradations of 65.4% and 89.5% were achieved in the sono-photocatalytic oxidation of CBZ at the frequencies of 20 and 850 kHz, respectively. The obtained higher degradations in sono-photocatalytic oxidation than that of photocatalytic oxidation at different stirring speeds is a good evidence of chemical effect of sonication on degradation of CBZ.

Effect of power (as power density) on sono-photocatalytic degradation of CBZ using low frequency (20 kHz) ultrasound (a) and high frequency (850 kHz) ultrasound (b) with an initial concentration of CBZ of 10 ppm, catalyst amount of 1 g/L, without pH regulation, and at a temperature of 298 K was also investigated in the present study. Fig. 13 presents this effect.

As seen in Fig. 13a, degradation percentage of CBZ increased from 65.4% to 79.3% and then to 84.4% with increasing power densities from 0.15 W/mL to 0.23 W/mL and then to 0.3 W/mL, respectively in low frequency ultrasonic system of 20 kHz, Fig. 13a. The same enhancement in degradation of CBZ was observed in high frequency ultrasonic system of 850 kHz, see Fig. 13b. The degradation of CBZ increased from 23.5% to 35.5% while increasing ultrasonic power density from 0.02 W/mL to 0.03 W/mL, respectively. The highest CBZ degradation of 89.5 % was achieved at power density of 0.12 W/mL.

In sonication, ultrasonic power can either be expressed as ultrasonic intensity (related to the transmitted area of ultrasound) or be expressed as power density (related to the solution volume). In the presented study the term of power density was used. The relationship between acoustic pressure (P_0) and power intensity (I) is given in Eq. (16):

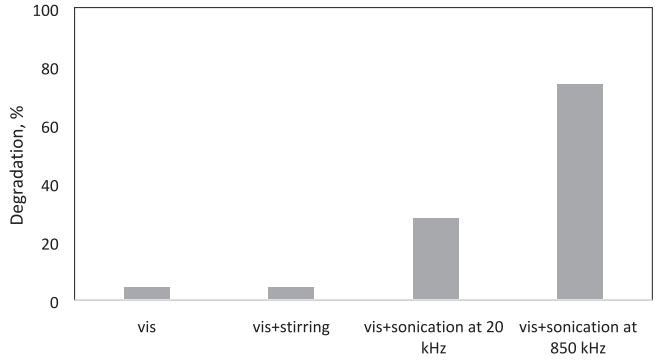

Fig. 11. Degradation of CBZ without photocatalyst with visible light under different conditions ($[CBZ]_0$ = 10 ppm, T = 298 K, without pH regulation, LED light power = 93.4 W, frequency = 20 kHz or 850 kHz, power density = 0.15 W/mL or 0.12 W/mL, continuous stirring of 1500 rpm).

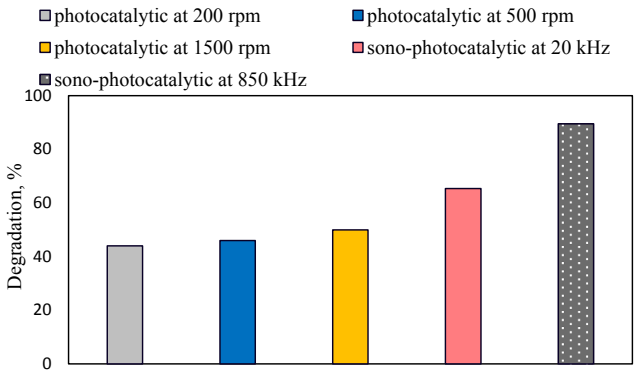

Fig. 12. Effect of stirring speed and sonication on degradation of CBZ ($[CBZ]_0$ = 10 ppm, T = 298 K, without pH regulation, LED light power = 93.4 W, frequency = 20 kHz or 850 kHz, power density = 0.15 W/mL or 0.12 W/mL, continuous stirring of 200, 500 and 1500 rpm).

$$I = P_0^2/2\rho C \tag{16}$$

Where ρ is the density of the liquid in kg m^{-3} and C is the velocity of the sound in liquid.

From Eq.16 it is clear that the acoustic pressure increases with the intensity (or power), and thus, the number of cavitation events increase. This increment causes more violent collapse of cavitation bubble releasing more reactive species available for the oxidation of organic pollutants. The increased power also leads to diffusion of organic pollutants from bulk solution to cavitation bubble–liquid interface due to the vibration of the pollutants in the bulk solution [68].

In the study done by Tran et al., 2013, sonochemical degradation of CBZ was studied at 520 kHz. The degradations of 41.9 %, 58.2 %, 58.5 %, and 58.7 % were achieved at powers of 10, 20, 30, and 40 W [13]. Frontistis and Mantzavinos 2012, investigated the sonochemical degradation of 17α-ethinylestradiol at a frequency of 80 kHz using different power densities of 18, 27, 41, and 46 W/L. They observed enhancement in degradation of 17α-ethinylestradiol with increasing power densities [71]. The removal efficiencies of sulfamethazine were 41.2 %, 68.2 %, 83.1 %, and 94.9 % under the ultrasonic powers of 40, 60, 80, and 100 W, respectively, at 800 kHz frequency within a reaction time of 60 min [72]. In another study done by Isariebel et al., 2009 [73], sonochemical degradation of acetaminophen and levodopa were carried out at powers of 9, 17, 22, and 32 W at a frequency of 574 kHz. They concluded that the degradation rate was increased with the power. Similar result was observed in sonochemical degradation of acetaminophen at a frequency of 600 kHz at four different powers of 20, 30, 40, 50, and 60 W. The degradation of acetaminophen was found to be increased with increasing power, and the highest degradation was achieved at 60 W [74]. In the study done by Wang et al. [75], sonochemical degradation of tetracycline (TC) was studied at a frequency of 20 kHz. The degradation ratio of TC were achieved as 67.4 %, 74.6 %, 79.2 %, 81.0 %, and 80.1 % under the ultrasonic powers of 100, 200, 300, 400, and 500 W, respectively. As known, an increase in ultrasonic power indicates that higher-intensity ultrasound was introduced into the reactor, and that would accelerate the reactions. However in their study, the increase in ultrasonic power led to the rise in degradation rate up to 400 W. Further increasing the power to 500 W led to decrease the degradation degree from 81.0 % to 80.1 %. They explained the increase in degradation with increasing power by providing more energy distributed to the reaction system to accelerate the cavitation effect. The amplification in acoustic power increased the number and the radius of the active cavitation bubbles. However, they mentioned that when ultrasonic intensity exceeded the optimal value, a large number of gas bubbles appeared in the solution. The coalescence of numerous

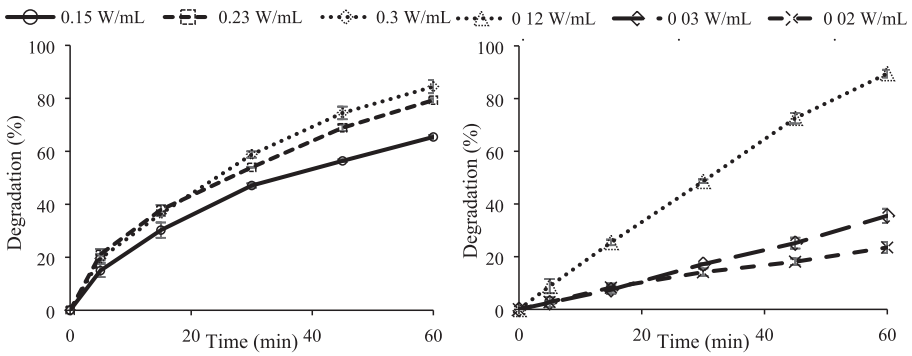

Fig. 13. Effect of power density of sonication in sono-photocatalytic oxidation of CBZ a) using low frequency (20 kHz) b) using high frequency (850 kHz) ultrasonic bath ($[CBZ]_0$ = 10 ppm, Catalyst loading = 1 g/L, T = 298 K, without pH regulation, and LED light power = 93.4 W, continuous stirring of 200 rpm).

cavitation bubbles may have resulted in the formation of a large cavity that collapses less violently. These large bubbles may also cause the scattering effect of the sound waves and thus provide a lower level of energy to be focused on the organic pollutant. Thus, with increased operating power, the utilization efficiency of the ultrasound decreased and degradation degree decreased.

Figure 14 shows the effect of sonication mode (continuous or pulse) on CBZ removal in high frequency (850 kHz) sonication system. The amplitude value was set as 75%, and the calculated acoustic power densities were measured as 0.12 W/mL, 0.029 W/mL, and 0.014 W/mL for continuous mode, and pulse mode sonication of 5:1, and 1:5, respectively. As seen in Fig. 14, the highest degradation of 89.5% was obtained in continuous mode after a reaction time of 60 min. It was followed by pulse mode with pulse duty ratio of 5:1. In that pulse duty ratio 54.0 % degradation of CBZ was achieved. The lowest degradation of 39.8 % was obtained for the pulse duty ratio of 1:5. It is clear that continuous mode of sonication was more effective than that of pulse mode in degradation of CBZ.

The degradation degree of organic pollutants under both continuous mode and pulse mode ultrasound depends on physicochemical properties, including molecular weight, molar volume, vapor pressure, log K_{OW}, and Henry's law constant. For example, hydrophobic compounds decompose faster due to the higher degree of accumulation on the hydrophobic cavitation bubble–liquid interface where the temperature is high enough for thermal pyrolysis and the number of active radicals are abundant for oxidation. Xiao et al. (2013) investigated the effect of ultrasound mode on degradation of several pharmaceuticals of carbamazepine (CBZ), ibuprofen (IBU), acetaminophen (ATP), sulfomethoxazole (SFT), and ciprofloxacin (CIPRO) and personal care products of propyl gallate (PG), and diethyl phthalate (DP). Although

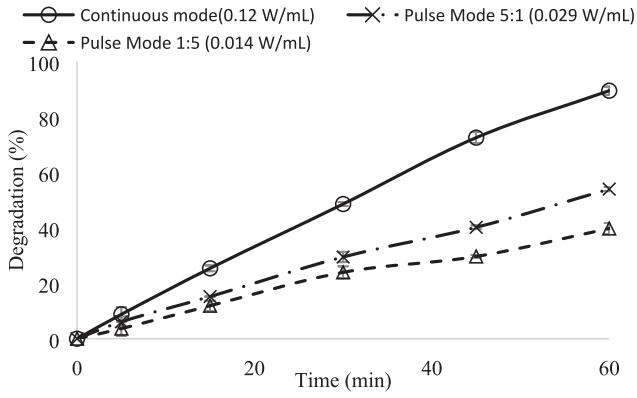

Fig. 14. Effect of sonication mode in sono-photocatalytic oxidation of CBZ using high frequency (850 kHz) ultrasonic reactor ($[CBZ]_0$ = 10 ppm, Catalyst loading = 1 g/L, T = 298 K, without pH regulation, and LED light power = 93.4 W, continuous stirring of 200 rpm).

they mentioned that there was no correlation between the degradation rate and any single property mentioned above, they observed positive pulse enhancement for small-sized (low molecular weight) pharmaceuticals, while large-sized (high molecular weight) pharmaceuticals exhibit a negative pulse enhancement. For example for the degradation of higher molecular weight (MW) compounds of SFT (MW = 253.28 g mol^{-1}) and CIPRO (MW = 331.34 g mol^{-1}) continuous mode of ultrasound was more efficient than that of pulse mode ultrasound. While, for the degradation of lower molecular weight compounds of ATP (MW = 151.17 g mol^{-1}) and IBU (MW = 208.28 g mol^{-1}) pulse mode ultrasound was more effective that of continuous mode. In that study, the sonochemical degradation of CBZ (MW = 236.37 g mol^{-1}) at pulse mode ultrasound was slightly higher than degradation in continuous mode [14].

3.4. Sono-catalytic oxidation of CBZ in simulated wastewater

The reuse of treated wastewater is imperative to meet the increasing global water demand for cleaning water. Regulations regarding the reuse and discharge of wastewater are strictly applied to municipal and industrial wastewater treatment plants. So it is important to investigate the efficiency of sono-catalytic oxidation for more complex water matrices containing inorganic ions and some natural organic materials (NOM) such as fulvic and humic acids. In this context, in the present study the sono-catalytic oxidation of CBZ was also conducted with simulated wastewater that contains some common anions in surface water such as, SO_4^{2-}, CO_3^{2-}, NO^{3-}, Cl^- and NOM of fulvic acid (FA). Experiments were done under the following conditions: 200 mL of 10 ppm CBZ solution, with 1 g/L of Ag/AgCl/$BiVO_4$ photocatalyst and 5 mM of anions or 0.05 mM of FA using high frequency (850 kHz) ultrasonic reactor at a power density of 0.12 W/mL on continuous mode without pH regulation. Na_2SO_4, Na_2CO_3, $NaNO_3$, and NaCl were used as source of SO_4^{2-}, CO_3^{2}, NO_3^-, and Cl^-, respectively. This effect is presented in Fig. 15.

As seen in Fig. 15, the effect inorganic ions in the CBZ degradation were different. The CBZ degradation was inhibited in the presence of NO_3^- and Cl^- from 72.9% to 65% and 70.8%, respectively. However, the existence of SO_4^{2-} and CO_3^{2-} increased the degradation degree of CBZ from 72.9% to 83.6% and 74.8%, respectively. Generally, two aspects, in the presence of anions, can impact the sono-catalytic oxidation. First, ions in water may cause a so-called "salting out effect" which push organic pollutant molecules from the bulk aqueous phase toward the bubble-bulk interface, that accelerated the degradation. Secondly, anions present in water act as scavenging agent of free radicals predominantly in the bulk water phase. However, the major reaction site for the hydrophobic compounds, such as CBZ, is the vapor phase of the cavitation bubbles and/or in the cavitation bubble - liquid interface but not the bulk aqueous phase. So the effect of NO_3^- and Cl^- were not so significant in the degradation of CBZ [44,75,72].

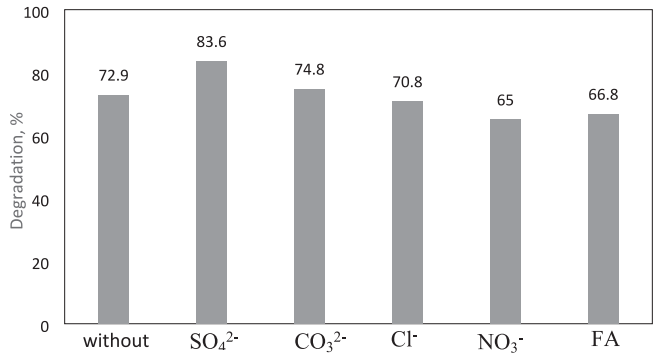

Fig. 15. Effects of different anions and fulvic acid on the sono-catalytic oxidation of CBZ using high frequency (850 kHz) ultrasonic reactor ($[CBZ]_0$ = 10 ppm, Catalyst loading = 1 g/L, T = 298 K, without pH regulation, power density = 0.12 W/mL, continuous stirring of 200 rpm).

When it comes to NOM of fulvic acid that used to simulate the real natural water, the result showed that the presence of fulvic acid (FA) slightly decreased the sono-catalytic oxidation of CBZ from 72.9% to 66.8 %. FA is typically present in surface water, and negatively affecting the physical and chemical reactions expected during the sono-catalytic oxidation due to important interferences with the reactive oxygen species formed during the sono-catalytic process. The slight activity decrease could be due to accumulation of fulvic acid on the surface of $Ag/AgCl/BiVO_4$ particles that blocks the active sites of catalyst. This accumulation may decrease the sonoluminescence effect of sonication which cause a decrease in the production of reactive oxygen species formed during the sonocatalytic process. The other reason that influenced the degradation negatively may because of the valance band holes quenching effect of FA [76,77,78].

3.5. Toxicty tests

Toxicity tests were performed to determine the toxicity of untreated CBZ solution, and treated CBZ solution by photocatalytic, and sono-photocatalytic oxidations. Experiments were performed for 10 ppm CBZ, at the catalyst loading of 1 g/L, at a temperature of 298 K, at neutral pH at power densities of 0.15 W/mL and 0.12 W/mL for ultrasonic probe system and ultrasonic reactor system, respectively within 60 min. Toxicty tests were conducted with measurement of root length of cress seeds (Lepidium Sativum L.). For this purpose, 20 seeds were put on the filter paper which placed in Petri dishes. They were prepared for untreated, and treated CBZ solution. Then, untreated and treated CBZ solution of 5 mL were dropped on Petri dishes contain seeds, and they were kept in dark cabinet for 120 h. At the end of 120 h, root length of cress seeds were measured. Toxicity reduction was measured taking the average root length of 20 seeds in each petri dishes according to equation given below [3,43,79,80]:

$$\text{Toxicityreduction}(\%) = \frac{\text{Rootlength}_{\text{treatedCBZ}} - \text{Rootlength}_{\text{untreatedCBZ}}}{\text{Rootlength}_{\text{treatedCBZ}}} \quad (17)$$

Toxicity reduction for the treated CBZ solution by photocatalytic,

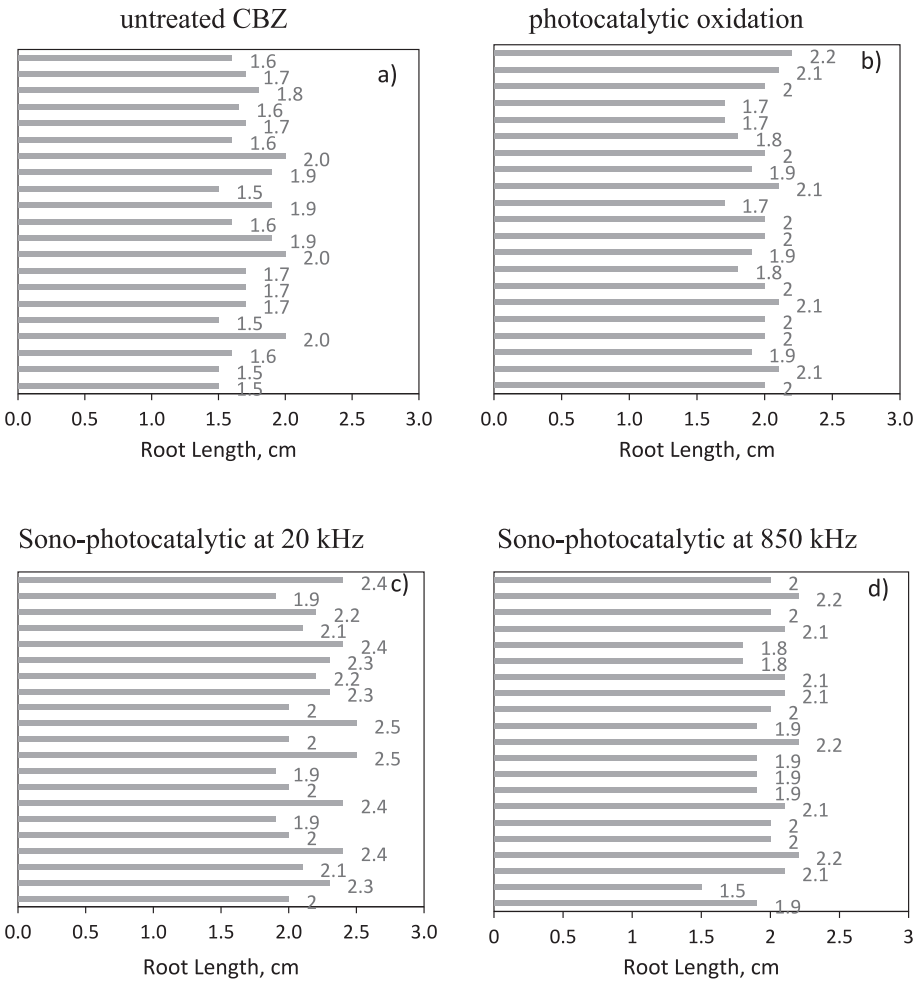

Fig. 16. Root length of cress seeds for untreated (a) and treated CBZ by photocatalytic (b) and sono-photocatalytic oxidation using ultrasonic probe (c) and ultrasonic reactor (d) systems.

and sono-photocatalytic oxidations using 20 kHz frequency probe (0.15 W/ml), and 850 kHz frequency ultrasonic reactor (0.12 W/mL) systems were measured as 12%, 14%, and 21.1%, respectively. Thus, it may say that the toxicity of treated CBZ solution by sono-photocatalytic oxidation using high frequency ultrasonic reactor was less than other processes. Fig. 16 shows the root length of each cress seeds for untreated, and treated CBZ solutions.

3.6. Economic analysis of hybrid oxidation processes

Costs of treatment of used hybrid oxidation processes were done using methodology reported in the references [81,82]. They have defined a parameter entitled "electric energy per order (EEO)", which represents the total cost of treatment. The EEO (kWh L^{-1} $order^{-1}$) is expressed by the Equation given below:

$$E_{EO} = \frac{1000*P*t}{V*\log\left(\frac{C_0}{C}\right)} \quad (18)$$

where P = the acoustic power (kW) for the sonication system and power of LED lamps for photocatalytic system, t = time of treatment (h), V = reaction volume (L), C_0 and C_f = the initial and final concentrations (mol/L) of CBZ, respectively. Table 7 presents the results. It could be seen that sono-photocatalytic oxidation in continuous mode had lower E_{E0} value of 599.7 kWhL^{-1}order^{-1} than that of pulse mode sono-photocatalytic and photocatalytic oxidation for ultrasonic reactor operated at 850 kHz. Similar result was obtained for ultrasonic probe system. If we have to compare the energy efficiency of the sono-photocatalytic hybrid process for ultrasonic reactor and ultrasonic probe systems, it appears that the ultrasonic reactor operating at 850 kHz has less cost of treatment, thus, has the highest potential for scale-up and commercialization. Further changing the operating reaction conditions, addition of small amount of green oxidants, such as hydrogen peroxide, peroxydisulfate or peroxymonosulfate may further reduce the treatment costs.

Sonication, an advanced oxidation process, has many advantages in the wastewater treatment technology. It need not require addition of the chemical additives. In contrast to many other processes which are negatively affected when suspended solids of effluent increase, US efficiency may even improve by increase of turbidity or suspended solids that act as nuclei for the formation of cavitation bubbles. In addition to these, as obtained in this study, if it is used combined with other AOPs, due to the synergetic effect, the degradation efficiencies could be increased significantly and the time required for complete degradation could be decreased. On the other hand, although sonication technology has shown to be feasible on a small scale application, the application of sonication in wastewater treatment on pilot-scale or industrial usage is still challenge, due to the high energy requirement of the process and operating costs linked to the maintenance and/or replacement of instruments which continue to be damaged by ultrasonic activity itself [83,84]. Considering the scarcity of water resources and the harmful effects of sewage on water bodies, water treatment is an important issue and the development of new water treatment techniques is inevitable. In this concern, it is thought that the results obtained from this study will lead to large-scale studies that can be done in the future. In literature there are some studies which used sonication as a pilot scale sludge pretreatment process [85,86] and pilot scale water disinfection system [87].

3.7. Comparison of results obtained from this study with other studies

The performance of AOPs used in the current study was compared with other treatments methods in literature in terms of removal of CBZ. The comparison data are presented in Table 8. It could be seen that, adsorption and visible light photocatalytic oxidation require long reaction time (2–3h) [88,89,93–95]. Hydrodynamic cavitation/UV/persulfate [82] and photoFenton [92] oxidation achieved high CBZ degradation for a reaction time of $\leq$ 1 h under UV-C light irradiation. As known well, UV-C light occupies only 5% of solar light. Microbial degradation and treatment in bioreactor were effective for removal of CBZ, however they require long treatment time [90]. The removal of CBZ by visible light photocatalytic oxidation over different photocatalysts were effective as achieved in the present study over Ag/AgCl/$BiVO_4$ photocatalyst. In the hybrid process of photoelectrocatalytic [91] oxidation complete degradation was achieved within 1.5 h. In the sono-catalytic oxidation of CBZ [96], almost complete degradation was obtained at high frequency of sonication (1000 kHz) that is similar result obtained in the current study at a frequency of 850 kHz. Although sonication was used with electrochemical treatment [97], 86.85% removal of CBZ was achieved within 3 h of reaction that strongly depends on the reaction and sonication parameters. As a conclusion, it could be said that Ag/AgCl/$BiVO_4$ was very effective in visible light photocatalytic oxidation, and sono-catalytic/sono-photocatalytic oxidation at high frequency of 850 kHz was efficient treatment process for CBZ removal relative to other reported processes.

4. Conclusions

This study aimed to investigate synergistic effect of sonication on optimized photocatalytic oxidation of pharmaceutical drug carbamazepine. In the photocatalytic oxidation, the parametric study was performed over Ag/AgCl/$BiVO_4$ photocatalyst and the effects of pH, catalyst loading and initial CBZ concentration on photocatalytic oxidation of CBZ were investigated. In order to optimize the conditions of photocatalytic oxidation, the response surface methodology was used in the Central Composite Design (CCD) of experiments. Complete carbamazepine removal was achieved at the optimum conditions of 5 ppm CBZ initial concentration with 1.5 g/L of catalysts loading and at an alkaline pH of 10 at the end of 4 h of reaction. It was found that, increment in catalyst amount and decrease in CBZ initial concentration increased the photocatalytic oxidation of CBZ. Increment in initial pH increased the photocatalytic degradation of CBZ. This increment is significant up to pH 8.5. After this pH, there was no significant change in

Table 7
Comparison of treatment costs for the processes used in the present study.

Treatment Process		US amplitude	Power, kW	Time, h	C_0,Mol L^{-1}	C, Mol L^{-1}	E_{E0} kWh L^{-1}order^{-1}
Reactor (850 kHz)	sonication	75%	0.024	1	$4.2*10^{-5}$	$1.1*10^{-5}$	211.0312
	Sono-catalytic	75%	0.024	1	$4.2*10^{-5}$	$1.1*10^{-5}$	211.0312
	photocatalytic	–	0.0934	1	$4.2*10^{-5}$	$2.4*10^{-5}$	1854.558
	Sono-photocatalytic (continous mode)	75%	0.1174	1	$4.2*10^{-5}$	$4.4*10^{-6}$	599.7074
	Sono-photocatalytic (pulse mode 1:5)	75%	0.09624	1	$4.2*10^{-5}$	$2.5*10^{-5}$	2183.268
	Sono-photocatalytic (pulse mode 5:1)	75%	0.0991	1	$4.2*10^{-5}$	$1.9*10^{-5}$	1469.271
Probe (20 kHz)	sonication	20%	0.03	1	$4.2*10^{-5}$	$3.1*10^{-5}$	1455.693
	Sono-catalytic	20%	0.03	1	$4.2*10^{-5}$	$3.04*10^{-5}$	1398.903
	photocatalytic	–	0.0934	1	$4.2*10^{-5}$	$2.4*10^{-5}$	2472.744
	Sono-photocatalytic	20%	0.1234	1	$4.2*10^{-5}$	$1.5*10^{-5}$	1784.821

Table 8
Comparison of results obtained from the present study with other studies in literatures for degradation of CBZ.

Treatment Methods	CBZ (ppm)	Catalyst/ adsorbent	Removal %	Ref.
Adsorption	1 mgL^{-1}	diatomaceous earth (DE) modified with iron-oxide	88.2 % (2 h).	[88]
Adsorption	5–25 mgL-1	Hematite nanoparticles	55 % (2.5 h)	[89]
Hydrodynamic cavitation /UV/ persulfate	15 mgL^{-1}	$ZnO/ZnFe_2O_4$	98.13 % (1 h)	[82]
Hydrodynamic cavitation	15 mgL^{-1}	–	7.70 % (1 h)	
Hydrodynamic cavitation + UV	15 mgL^{-1}	–	22.27 % (1 h)	
Hydrodynamic cavitation + persulfate	15 mgL^{-1}	–	65.73 % (1 h)	
Hydrodynamic cavitation + $ZnFe_2O_4$	15 mgL^{-1}	$ZnO/ZnFe_2O_4$	18.29 % (1 h)	
UV + $ZnFe_2O_4$	15 mgL^{-1}		42.49 % (1 h)	
Hydrodynamic cavitation + UV + $ZnFe_2O_4$	15 mgL^{-1}	$ZnO/ZnFe_2O_4$	53.26 % (1 h)	
Microbial degradation	175 μgL^{-1}	–	77% (6 h)	[90]
Forward osmotic membrane bioreactor	200 μgL^{-1}	–	~90 % (80 days)	
Photoelectrocatalytic	5 mgL^{-1}	Reduced TiO_2 NTAs photoanode and activated carbon/ Polytetrafluoroethylene (AC/PTFE) cathode	~100% (1.5 h)	[91]
PhotoFenton	23 mgL^{-1}	FeOCl	92% (0.5 h)	[92]
Visible light Photocatalytic	50 mgL^{-1}	BiOCl and BiOCl/AgCl	80% and 60% over BiOCl/AgCl and BiOCl, (3 h)	[93]
Visible light Photocatalytic	2.5 mgL^{-1}	BiOCl with different Bi $(NO_3)_3$/KCl	70% with BiOCl-10 sample (3 h)	[94]
Visible light Photocatalytic	10 mgL^{-1}	biochar-based magnetic photocatalyst Fe_3O_4/ BiOBr/BC (with different biochar mass ratios)	95.51% with Fe_3O_4/ BiOBr/BC10 (3 h)	[95]
Sono-catalytic		Metal Organic Framework (MOF)	at 28 kHz 25% (only US)at 28 kHz 47% (US/MOF) at 1000 kHz 97% (only US)at 1000 kHz 99% (US/MOF) (1 h)	[96]
Sonoelectrochemical	1.5 mgL^{-1}	two concentrical electrodes	86.85 % (3 h)	[97]
Visible light photocatalytic	5 mgL^{-1}	$Ag/AgCl/BiVO_4$	100 % (3 h)	Present study
Sono-catalytic	10 mgL^{-1}	$Ag/AgCl/BiVO_4$	at 20 kHz 28.1% (1 h) at 850 kHz 72.9% (1 h)	
Sono-photocatalytic	10 mgL^{-1}	$Ag/AgCl/BiVO_4$	at 20 kHz 65.4% (1 h) at 850 kHz 89.5% (1 h)	

degradation with pH of CBZ solution. In the kinetic study, at different temperatures of 298, 303, 308, and 313 K, the photocatalytic oxidation of CBZ was described by the first order kinetics with an activation energy of 10.6 kJ/mol. The temperature of 308 K was found as optimum temperature with 93.37 % of CBZ degradation and 10.77% of TOC reduction under the following conditions of $[CBZ]_0 = 10$ ppm, Catalyst loading = 1 g/L, pH = 7, LED light power = 93.4 W.

Effect of sonication experiments exhibited that in the low frequency ultrasonic system (20 kHz), CBZ removal increased from 44 % to 65.42 % and in the high frequency ultrasonic system (850 kHz) CBZ removal increased from 44 % to 89.5 % within 60 min of reaction. Continuous mode of sonication was more favorable than that of pulse mode sonication. Synergistic effect between photocatalytic oxidation and sonication was investigated at low frequency probe system and also at high frequency (850 kHz) ultrasonic reactor. The result shows that 18.7 % and 4.04 % of synergistic effects were observed between sono-catalytic oxidation and photocatalytic oxidation at low frequency and high frequency sonication, respectively. Ultrasonic reactor operated at 850 kHz had less cost of treatment of CBZ than that of ultrasonic probe system. Sono-catalytic oxidation conducted with simulated wastewater that contains SO_4^{2-}, CO_3^{2-}, NO^{3-},Cl^- anions and natural organic material of fulvic acid showed two different results. The CBZ degradation decreased slightly in the presence of NO_3^- and Cl^-, and fulvic acid, however, the existence of SO_4^{2-} and CO_3^{2-} increased the degradation degree of CBZ. Toxicity tests were performed to determine the toxicity of untreated CBZ, and treated CBZ by photocatalytic, and sono-photocatalytic oxidation. It was observed that, toxicity of CBZ solution treated by sono-photocatalytic oxidation was less than of photocatalytic oxidation.

CRediT authorship contribution statement

Gizem Yentür: Investigation. **Meral Dükkancı:** Supervision, Project administration, Funding acquisition.

Declaration of Competing Interest

The authors declare that they have no known competing financial interests or personal relationships that could have appeared to influence the work reported in this paper.

Acknowledgements

The authors are grateful the financial support from TÜBİTAK (The Scientific and Technological Research Council of Turkey) under project number of 218M616. We appreciate Prof. Dr. Gönül Gündüz for guiding us during this study.

References

[1] J. Theerthagiri, S.J. Lee, K. Karuppasamy, S. Arulmani, S. Veeralakshmi, M. Ashokkumar, M.Y. Choi, Application of advanced materials in sonophotocatalytic processes for the remediation of environmental pollutants, J. Hazard. Mater. 412 (2021), 125245.
[2] A.G. Ramu, L. Telmenbayar, J. Theerthagiri, G. Yang, M. Song, G. Choi, Synthesis of a hierarchically structured Fe_3O_4–PEI nanocomposite for the highly sensitive electrochemical determination of bisphenol A in real samples, New J. Chem. 44 (2020) 18633.
[3] G. Yentür, M. Dükkancı, Fabrication of magnetically separable plasmonic composite photocatalyst of $Ag/AgBr/ZnFe_2O_4$ for visible light photocatalytic oxidation of carbamazepine, Appl. Surf. Sci. 510 (2020), 145374.
[4] F.I. Hai, S. Yang, M.B. Asif, V. Sencadas, S. Shawkat, M. Sanderson-Smith, J. Gorman, Z.-Q. Xu, K. Yamamoto, Carbamazepine as a possible anthropogenic marker in water: occurrences, toxicological effects, regulations and removal by wastewater treatment technologies, Water 10 (107) (2018) 1–32.
[5] K. Dwivedi, A. Morone, V. Pratape, T. Chakrabarti, R.A. Pandey, Carbamazepine and oxcarbazepine removal in pharmaceutical wastewater treatment plant using a mass balance approach: a case study, Korean J. Chem. Eng. 34 (2017) 3662–12671.
[6] J. Theerthagiri, J. Madhavan, S.J. Lee, M.Y. Choi, M. Ashokkumar, B.G. Pollet, Sonoelectrochemistry for energy and environmental applications, Ultrason Sonochem. 63 (2020), 104960.

[7] F. Ali, L. Reinert, J.M. Lévêque, L. Duclaux, F. Muller, S. Saeed, S.S. Shah, Effect of sonication conditions: solvent, time, temperature and reactor type on the preparation of micron sized vermiculite particles, Ultrason Sonochem. 21 (3) (2014) 1002–1009.

[8] M. Dükkancı, M. Vinatoru, T.J. Mason, The sonochemical decolourisation of textile azo dye Orange II: effects of Fenton type reagents and UV light, Ultrason Sonochem. 21 (2014) 846–853.

[9] M. Dükkancı, Sono-photo-Fenton oxidation of bisphenol-A over a $LaFeO_3$ perovskite catalyst, Ultrason Sonochem. 40 (2018) 110–116.

[10] K. González Labrada, D.R. Alcorta Cuello, I. Saborit Sánchez, M. García Batle, M. H. Manero, L. Barthe, U.J. Jáuregui-Haza, Optimization of ciprofloxacin degradation in wastewater by homogeneous sono-Fenton process at high frequency, J. Environ. Sci. Health A 53 (13) (2018) 1139–1148.

[11] S. Khan, M. Sayed, M. Sohail, L.A. Shah, M.A. Raja. Advanced oxidation and reduction processes, Adv. Water Purification Techn. Elsevier, 2019 135-164.

[12] D. Kanakaraju, B.D. Glass, M. Oelgemöller, Advanced oxidation process-mediated removal of pharmaceuticals from water: a review, J. Environ. Manage. 219 (2018) 189–207.

[13] N. Tran, P. Drogui, F. Zaviska, S.K. Brar, Sonochemical degradation of the persistent pharmaceutical carbamazepine, J. Environ. Manage. 131 (2013) 25–32.

[14] R. Xiao, D. Diaz-Rivera, L.K. Weavers, Factors influencing pharmaceutical and personal care product degradation in aqueous solution using pulsed wave ultrasound, I&EC Res. 52 (2013) 2824–2831.

[15] J. Madhavan, J. Theerthagiri, D. Balaji, S. Sunitha, M.Y. Choi, M. Ashokkumar, Hybrid advanced oxidation processes involving ultrasound: an overview, Molecules 24 (3341) (2019) 1–18.

[16] J. Theerthagiri, R.A. Senthil, B. Senthilkumar, A.R. Polu, J. Madhavan, M. Ashokkumar, Recent advances in MoS_2 nanostructured materials for energy and environmental applications – A review, J. Solid State Chem. 252 (2017) 43–71.

[17] T. Jayaraman, A.P. Murthy, V. Elakkiya, S. Chandrasekaran, P. Nithyadharseni, Z. Khan, R.A. Senthil, R. Shanker, M. Raghavender, P. Kuppusami, M. Jagannathan, M. Ashokkumar, Recent development on carbon based heterostructures for their applications in energy and environment: a review, J. Ind. Eng. Chem. 64 (2018) 16–59.

[18] J. Theerthagiri, S. Salla, R.A. Senthil, P. Nithyadharseni, A. Madankumar, P. Arunachalam, T. Maiyalagan, H.S. Kim, A review on ZnO nanostructured materials: energy, environmental and biological applications, Nanotechnology 30 (392001) (2019) 1–27.

[19] M. Liu, L.A. Hou, B.D. Xi, Q. Li, X. Hu, S. Yu, Magnetically separable Ag/AgCl-zero valent iron particles modified zeolite X heterogeneous photocatalysts for tetracycline degradation under visible light, Chem. Eng. J. 302 (2016) 475–484.

[20] B. Shi, H. Yin, J. Gong, Q. Nie, Ag/AgCl decorated $Bi_4Ti_3O_{12}$ nanosheet with highly exposed (001) facets for enhanced photocatalytic degradation of Rhodamine B, Carbamazepine and Tetracycline, Appl. Surf. Sci. 419 (2017) 614–623.

[21] Y. Zhu, R. Zhu, Y. Xi, T. Xu, L. Yan, J. Zhu, G. Zhu, H. He, Heterogeneous photo-Fenton degradation of bisphenol A over Ag/AgCl/ferrihydrite catalysts under visible light, Chem. Eng. J. 346 (2018) 567–577.

[22] Q. Liu, Y. Xu, J. Wang, M. Xie, W. Wei, L. Huang, H. Xu, Y. Song, H. Li, Fabrication of Ag/AgCl/$ZnFe_2O_4$ composites with enhanced photocatalytic activity for pollutant degradation and E. coli disinfection, Colloid Surface A 553 (2018) 114–124.

[23] H. Li, Y. Sun, B. Cai, S. Gan, D. Han, L. Niu, T. Wu, Hierarchically Z-scheme photocatalyst of Ag@AgCl decorated on $BiVO_4$ (040) with enhancing photoelectrochemical and photocatalytic performance, Appl. Catal. B-Environ. 170 (2015) 206–214.

[24] R. Qiao, M. Mao, E. Hu, Y. Zhong, J. Ning, Y. Hu, Facile formation of mesoporous $BiVO_4$/Ag/AgCl heterostructured microspheres with enhanced visible-light photoactivity, Inorg. Chem. 54 (18) (2015) 9033–9039.

[25] F. Chen, C. Wu, J. Wang, C.P. François-Xavier, T. Wintgens, Highly efficient Z-scheme structured visible-light photocatalyst constructed by selective doping of Ag@ AgBr and Co3O4 separately on 010 and 110 facets of BiVO4: pre-separation channel and hole-sink effects, Appl. Catal. B-Environ. 250 (2019) 31–41.

[26] R. Akbarzadeh, C.S. Fung, R.A. Rather, I.M. Lo, One-pot hydrothermal synthesis of g-C_3N_4/Ag/AgCl/$BiVO_4$ micro-flower composite for the visible light degradation of ibuprofen, Chem. Eng. J. 341 (2018) 248–261.

[27] Z. Zhou, M. Long, W. Cai, J. Cai, Synthesis and photocatalytic performance of the efficient visible light photocatalyst Ag–AgCl/$BiVO_4$, J. Mol. Catal. A-Chem. 353 (2012) 22–28.

[28] L. Tang, J.J. Wang, C.T. Jia, G.X. Lv, G. Xu, W.T. Li, L. Wang, J.Y. Zhang, M.H. Wu, Simulated solar driven catalytic degradation of psychiatric drug carbamazepine with binary $BiVO_4$ heterostructures sensitized by graphene quantum dots, Appl. Catal. B-Environ. 205 (2017) 587–596.

[29] R. Li, F. Zhang, D. Wang, J. Yang, M. Li, J. Zhu, X. Zhou, H. Han, C. Li, Spatial separation of photogenerated electrons and holes among 010 and 110 crystal facets of BiVO4, Nat. Commun. 4 (2013) 1432.

[30] M.A.N. Khan, M. Siddique, F. Wahid, R. Khan, Removal of reactive blue 19 dye by sono, photo and sonophotocatalytic oxidation using visible light, Ultrason Sonochem. 26 (2015) 370–377.

[31] V.K. Mahajan, S.P. Patil, S.H. Sonawane, G.H. Sonawane, Ultrasonic, photocatalytic and sonophotocatalytic degradation of Basic Red-2 by using Nb_2O_5 nano catalyst, Biophysics 3 (2016) 415–430.

[32] E. Selli, Synergistic effects of sonolysis combined with photocatalysis in the degradation of an azo dye, Phys. Chem. Chem. Phys. 4 (24) (2002) 6123–6128.

[33] J. Shah, M.R. Jan, F. Khitab, Sonophotocatalytic degradation of textile dyes over Cu impregnatedZnO catalyst in aqueous solution, Process Saf. Environ. 116 (2018) 149–158.

[34] S. Kumawat, K. Meghwal, S. Kumar, R. Ameta, C. Ameta, Kinetics of sonophotocatalytic degradation of an anionic dye nigrosine with doped and undoped zinc oxide, Water Sci. Technol. 80 (2019) 1466–1475.

[35] Y. Kristianto, A. Taufik, R. Saleh, Photo-, sono- and sonophotocatalytic degradation of methylene blue using Fe3O4/ZrO2 composites catalysts, Int. Sympos. Curr. Prog. Math. Sci. 3001 (2016) 1–6.

[36] M. Ahmad, E. Ahmed, Z.L. Hong, W. Ahmed, A. Elhissi, N.R. Khalid, Photocatalytic, sonocatalytic and sonophotocatalytic degradation of Rhodamine B using ZnO/CNTs composites photocatalysts, Ultrason Sonochem. 21 (2014) 761–773.

[37] M. Zargazi, M.H. Entezari, Sonochemical versus hydrothermal synthesis of bismuth tungstate nanostructures: photocatalytic, sonocatalytic and sonophotocatalytic activities, Ultrason Sonochem. 51 (2019) 1–11.

[38] T. Selvamani, S. Anandan, A.M. Asiri, P. Maruthamuthu, M. Ashokkum, Preparation of MgTi2O5 nanoparticles for sonophotocatalytic degradation of triphenylmethane dyes, Ultrason Sonochem. (2021) in press.

[39] G. Eshaq, A.E. ElMetwally, Bmim[OAc]-Cu2O/g-C3N4 as a multi-function catalyst for sonophotocatalytic degradation of methylene blue, Ultrason Sonochem. 53 (2019) 99–109.

[40] V. Vinesh, M. Ashokkumar, B. Neppolian, rGO supported self-assembly of 2D nano sheet of (g-C3N4) into rod-like nano structure and its application in sonophotocatalytic degradation of an antibiotic, Ultrason Sonochem. 68 (2020), 105218.

[41] D. Meronia, M. Jiménez-Salcedo, E. Falletta, B.M. Bresolin, C.F. Kait, D.C. Boffito, C.L. Bianchi, C. Pirol, Sonophotocatalytic degradation of sodium diclofenac using low power ultrasound and micro sized TiO2, Ultrason Sonochem. 67 (2020), 105123.

[42] L. Liang, Y. Tursun, A. Nulahong, T. Dilinuer, A. Tunishaguli, G. Gao, A. Abulikemu, K. Okitsu, Preparation and sonophotocatalytic performance of hierarchical Bi2WO6 structures and effects of various factors on the rate of Rhodamine B degradation, Ultrason Sonochem. 39 (2017) 93–100.

[43] G. Yentür, M. Dükkancı, Synthesis of Visible-Light heterostructured photocatalyst of Ag/AgCl deposited on (040) facet of monoclinic $BiVO_4$ for efficient carbamazepine photocatalytic removal, Appl. Surf. Sci. 531 (2020), 147322.

[44] M. Dükkancı, Heterogeneous sonocatalytic degradation of Bisphenol-A and the influence of the reaction parameters and ultrasonic frequency, Water Sci. Technol. 79 (2) (2019) 386–397.

[45] S.H. Hasan, P. Srivastava, M. Talat, Biosorption of Pb (II) from water using biomass of Aeromonas hydrophila: central composite design for optimization of process variables, J. Hazard. Mater. 168 (2–3) (2009) 1155–1162.

[46] P. Hashemi, F. Raeisi, A.R. Ghiasvand, A. Rahimi, Reversed-phase dispersive liquid–liquid microextraction with central composite design optimization for preconcentration and HPLC determination of oleuropein, Talanta 80 (5) (2010) 1926–1931.

[47] X. Zhang, R. Wang, X. Yang, J. Yu, Central composite experimental design applied to the catalytic aromatization of isophorone to 3, 5 xylenol, Chemometr. Intell. Lab. 89 (1) (2007) 45–50.

[48] M. Dükkancı, Photocatalytic Oxidation of Rhodamine 6G Dye Using Magnetic TiO_2@Fe_3O_4/FeZSM-5, Chem. Biochem. Eng. Q. 35 (2021) 17–29.

[49] L. Bo, H. Liu, H. Han, Photocatalytic degradation of trace carbamazepine in river water under solar irradiation, J. Environ. Manage. 241 (2019) 131–137.

[50] L. Dong, T. Xu, W. Chen, W. Lu, Synergistic multiple active species for the photocatalytic degradation of contaminants by imidazole-modified g-C_3N_4 coordination with iron phthalocyanine in the presence of peroxymonosulfate, Chem. Eng. J. 357 (2019) 198–208.

[51] H. Chen, X. Wang, W. Bi, Y. Wu, W. Dong, Photodegradation of carbamazepine with BiOCl/Fe_3O_4 catalyst under simulated solar light irradiation, J. Colloid Interf. Sci. 502 (2017) 89–99.

[52] Z. Hu, X. Cai, Z. Wang, S. Li, Z. Wang, X. Xie, Construction of carbon-doped supramolecule-based g-C_3N_4/TiO_2 composites for removal of diclofenac and carbamazepine: a comparative study of operating parameters, mechanisms, degradation pathways, J. Hazard. Mater. 380 (2019), 120812.

[53] T.B. Nguyen, C.P. Huang, R.A. Doong, Photocatalytic degradation of bisphenol A over a $ZnFe_2O_4$/TiO_2 nanocomposite under visible light, Sci. Total Environ. 646 (2019) 745–756.

[54] H.A. Ghaly, A.S. El-Kalliny, T.A. Gad-Allah, N.E.A. El-Sattar, E.R. Souaya, Stable plasmonic Ag/AgCl–polyaniline photoactive composite for degradation of organic contaminants under solar light, RSC Adv. 7 (21) (2017) 12726–12736.

[55] L. Yang, L. Liang, L. Wang, J. Zhu, S. Gao, X. Xia, Accelerated photocatalytic oxidation of carbamazepine by a novel 3D hierarchical protonated g-C_3N_4/BiOBr heterojunction: performance and mechanism, Appl. Surf. Sci. 473 (2019) 527–539.

[56] S. Begum, M. Ahmaruzzaman, CTAB and SDS assisted facile fabrication of SnO_2 nanoparticles for effective degradation of carbamazepine from aqueous phase: a systematic and comparative study of their degradation performance, Water Res. 129 (2018) 470–485.

[57] M. Dükkancı, Treatment of Bisphenol-A using sonication-assisted photo-Fenton hybrid process: influence of reaction parameters, Chem. Biochem. Eng. Q 33 (2019) 43–57.

[58] B. Krishnakumar, M. Swaminathan, Photodegradation of Acid Violet 7 with AgBr–ZnO under highly alkaline conditions, Spectrochim. Acta Part A Mol. Biomol. Spectrosc. 99 (2012) 160–165.

[59] F. Zhang, X. Wang, H. Liu, C. Liu, Y. Wan, Y. Long, Z. Cai, Recent advances and applications of semiconductor photocatalytic technology, Appl. Sci. 9 (12) (2019) 2489.

[60] A. Chatzitakis, C. Berberidou, I. Paspaltsis, G. Kyriakouc, T. Sklaviadis, I. Poulios, Photocatalytic degradation and drug activity reduction of Chloramphenicol, Water Res. 42 (2008) 386–394.
[61] E.T. Soares, M.A. Lansarin, C.C. Moro, A study of process variables for the photocatalytic degradation of Rhodamine B, Braz. J. Chem. Eng. 24 (1) (2007) 29–36.
[62] K.M. Reza, A.S.W. Kurny, F. Gulshan, Parameters affecting the photocatalytic degradation of dyes using TiO_2: a review, Appl. Water Sci. 7 (4) (2017) 1569–1578.
[63] S. Sarkar, R. Das, H. Choi, C. BhattacharjeFetyan, Involvement of process parameters and various modes of application of TiO_2 nano particles in heterogeneous photocatalysis of pharmaceutical wastes – A short review, RSC Adv. 4 (2014) 57250–57266.
[64] F. Shahrezaei Y. Mansouri A.A.L. Zinatizadeh A. Akhbari. Photocatalytic degradation of aniline using TiO2 nanoparticles in a vertical circulating photocatalytic reactor, Int. J. Photoenergy 2012 Article ID 430638, 1-8.
[65] X. Gao, Q. Guo, G. Tang, W. Zhu, Y. Luo, Controllable synthesis of solar-light-driven BiOCl nanostructures for highly efficient photocatalytic degradation of carbamazepine, J. Solid State Chem. 277 (2019) 133–138.
[66] S.G. Babu, P. Karthik, M.C. John, S.K. Lakhera, M. Ashokkumar, J. Khim, B. Neppolian, Synergistic effect of sono-photocatalytic process for the degradation of organic pollutants using CuO-TiO_2/rGO, Ultrason Sonochem. 50 (2019) 218–223.
[67] M. Dükkancı, M. Vinatoru, T.J. Mason, Sonochemical treatment of orange II using ultrasound at a range of frequencies and powers, J. Adv. Oxid. Technol. 15 (2012) 277–283.
[68] M.P. Rayaroth, U.K. Aravind, C.T. Aravindakumar. Degradation of pharmaceuticals by ultrasound-based advanced oxidation process, Environ. Chem. Lett. 14 2016 259–290.
[69] J. Choi, M. Cui, Y. Lee, J. Kim, Y. Yoon, M. Jang, J. Khim, Synthesis, characterization and sonocatalytic applications of nano-structured carbon based TiO_2 catalysts, Ultrason Sonochem. 43 (2018) 193–200.
[70] O.S. Ayanda, S.M. Nelana, E.B. Naidoo, Ultrasonic degradation of aqueous phenolsulfonphthalein (PSP) in the presence of nano-Fe/H_2O_2, Ultrason Sonochem. 47 (2018) 29–35.
[71] Z. Frontistis, D. Mantzavinos, Sonodegradation of 17 α –ethynylestradiol in environmentllly relevant matrices: laboratory-scale kinetic studies, Ultrason Sonochem. 19 (2012) 77–84.
[72] Y.Q. Gao, N.Y. Gao, Y. Deng, J.S. Gu, Y.L. Gu, D. Zhang, Factor affecting sonolytic degradation of sulfamethazine in water, Ultrason Sonochem. 20 (2013) 1401–1407.
[73] Q.P. Isariebel, J.L. Carine, J.H. Ulises-Javier, Sonolysis of levodopa and paracetamol in aqueous solutions, Ultrason Sonchem. 16 (2009) 610–616.
[74] E. Villaroel, J. Silva-Agredo, C. Petrier, G. Taborda, R.A. Torres-Palma, Ultrasonic degradation of acetaminophen in water: effect of sonochemical parameters and water matrix, Ultrason Sonochem. 21 (2014) 1763–1769.
[75] X. Wang, Y. Wang, D. Li, Degradation of tetracycline in water by ultrasonic irradiation, Water Sci. Technol. 67 (4) (2013) 715–721.
[76] I. Altin, X. Ma, V. Boffa, E. Bacaksız, G. Magnacca, Hydrothermal preparation of B-TiO2-graphene oxide ternary nanocomposite, characterization and photocatalytic degradation of bisphenol A under simulated solar irradiation, Mater. Sci. Semicond. Process. 123 (2021), 105591.
[77] G. Divyapriya, S. Singh, C.A. Martínez-Huitle, J. Scaria, A.V. Karim, P.V. Nidheesh, Treatment of real wastewater by photoelectrochemical methods: an overview, Chemosphere 276 (2021), 130188.
[78] M.G. Alalm, R. Djellabi, D. Meroni, C. Pirola, C.L. Bianchi, D.C. Boffito, Toward scaling-up photocatalytic process for multiphase environmental applications, Catalysts 11 (2021) 562.
[79] N. Demir, G. Gündüz, M. Dükkancı, Degradation of a textile dye, Rhodamine 6G (Rh6G), by heterogeneous sonophotoFenton process in the presence of Fe containing TiO_2 catalysts, Environ. Sci. Pollut. R. 22 (2015) 3193–3201.
[80] M.B. Arambasic, S. Bjelic, G. Subakov, Acute toxicity of heavy metals (copper, lead, zinc), phenol and sodium on Allium Cepa L., Lepedium Stavum L. and Daphnia Magna St.: comparative investigations and the practical applications, Water Res. 29 (1995) 497–503.
[81] J.R. Bolton, K.G. Bircher, W. Tumas, C.A. Tolman, Figures-of-merit for the technical development and application of advanced oxidation technologies for both electric-and solar-driven systems (IUPAC Technical Report), Pure Appl. Chem. 73 (2001) 627–637.
[82] R. Roy, V.S. Moholkar, Mechanistic analysis of carbamazepine degradation in hybrid advanced oxidation process of hydrodynamic cavitation/UV/persulfate in the presence of ZnO/ZnFe2O4, Sep. Purif. Technol. 270 (2021), 118764.
[83] A.H. Mahvi. Application of ultrasonic technology for water and wastewater treatment, Iranian J. Publ. Health 38 2010 1-17.
[84] N.A.H. Fetyan, T.M.S. Attia, Water purification using ultrasound waves: application and challenges, Arab. J. Basic Appl. Sci. 27 (2020) 194–207.
[85] N.T. Le, C. Julcour-Lebigue, H. Henri Delmas, An executive review of sludge pretreatment by sonication, J. Environ. Sci. 37 (2015) 139–153.
[86] T. Lippert, J. Bandelin, D. Vogl, Z.A. Tesieh, T. Wild, J.E. Drewers, K. Koch, Full-scale assessment of ultrasonic sewage sludge pretreatment using a novel double-tube reactor, ACS EST Engg. 1 (2021) 298–309.
[87] A. Hulsmans, K. Joris, N. Lambert, H. Rediers, P. Declerck, Y. Delaedt, F. Ollevier, S. Liers, Evaluation of process parameters of ultrasonic treatment of bacterial suspensions in a pilot scale water disinfection system, Ultrason Sonochem. 17 (2010) 1004–1009.
[88] S. Jemutai-Kimosop, F. Orata, V.O. Shikuku, V.A. Okello, Z.M. Geteng, Insights on adsorption of carbamazepine onto iron oxide modified diatomaceous earth: kinetics, isotherms, thermodynamics, and mechanisms, Environ. Res. 180 (2020), 108898.
[89] K. Rajendran, S. Sen, Adsorptive removal of carbamazepine using biosynthesized hematite nanoparticles, Environ. Nanotechnol. Monit. Manag. 9 (2018) 122–127.
[90] M. Yao, L. Duana, J. Wei, F. Qian, S.W. Hermanowicz, Carbamazepine removal from wastewater and the degradation mechanism in a submerged forward osmotic membrane bioreactor, Bioresour. Technol. 314 (2020), 123732.
[91] R. Guo, L.C. Nengzi, Y. Chen, Q. Song, J. Gou, X. Cheng, Construction of high-efficient visible photoelectrocatalytic system for carbamazepine degradation: kinetics, degradation pathway and mechanism, Chinese Chem. Lett. 31 (2020) 2661–2667.
[92] S. Sun, H. Yao, W. Fu, F. Liu, X. Wang, W. Zhang, Enhanced degradation of carbamazepine in FeOCl based Photo-Fenton reaction, J. Environ. Chem. Eng. 9 (2021), 104501.
[93] R. Meribout, Y. Zuo, A.A. Khodja, A. Piram, S. Lebarillier, J. Cheng, C. Wang, P. Wong-Wah-Chung, Photocatalytic degradation of antiepileptic drug carbamazepine with bismuth oxychlorides (BiOCl and BiOCl/AgCl composite) in water: efficiency evaluation and elucidation degradation pathways, J. Photoch. Photobio. A 328 (2016) 105–113.
[94] X. Gao, W. Peng, G. Tang, Q. Guo, Y. Luo, Highly efficient and visible-light-driven BiOCl for photocatalytic degradation of carbamazepine, J. Alloy. Compd. 757 (2018) 455–465.
[95] S. Li, Z. Wang, X. Zhao, X. Yang, G. Liang, X. Xie, Insight into enhanced carbamazepine photodegradation over biochar-based magnetic photocatalyst Fe_3O_4/BiOBr/BC under visible LED light irradiation, Chem. Eng. J. 360 (2019) 600–611.
[96] B.M. Jun, S. Kim, J. Heob, N. Her, M. Jang, Park, C.M. Yeomin Yoon, Enhanced sonocatalytic degradation of carbamazepine and salicylic acid using a metal-organic framework, Ultrason Sonochem. 56 (2019) 174–182.
[97] N. Tran, P. Drogui, S.K. Brar, Sonoelectrochemical oxidation of carbamazepine in waters: optimization using response surface methodology, J. Chem. Technol. Biotechnol. 90 (2015) 921–929.